

Temporal Action Segmentation: An Analysis of Modern Technique

Guodong Ding*, Fadime Sener*, and Angela Yao

Abstract—Temporal action segmentation from videos aims at the dense labeling of video frames with multiple action classes in minutes-long videos. Categorized as a long-range video understanding task, researchers have proposed an extended collection of methods and examined their performance using various benchmarks. Despite the rapid development of action segmentation techniques in recent years, there has been no systematic survey in such fields. To this end, in this survey, we analyse and summarize the main contributions and trends for this task. Specifically, we first examine the task definition, common benchmarks, types of supervision and popular evaluation measures. Furthermore, we systematically investigate two fundamental aspects of this topic, *i.e.*, frame representation and temporal modeling, which are widely and extensively studied in the literature. We then comprehensively review existing temporal action segmentation works, each categorized by their form of supervision. Finally, we conclude our survey by highlighting and identifying several open topics for research. In addition, we supplement our survey with a curated list of temporal action segmentation resources, which is available at <https://github.com/atlas-eccv22/awesome-temporal-action-segmentation>.

Index Terms—Artificial Intelligence, Computer Vision, Video Understanding, Temporal Action Segmentation, Video Representation, Temporal & Sequential Modeling, Literature Survey



1 INTRODUCTION

TEMPORAL action segmentation (TAS) is a video understanding task that segments in time a temporally untrimmed video sequence. Each segment is labeled with one of a finite set of pre-defined action labels (see Fig. 1 for a visual illustration). This task is a 1D temporal analogue to the more established semantic segmentation [1], replacing pixel-wise semantic labels to frame-wise action labels. Automatically segmenting untrimmed video sequences helps to understand what actions are being performed, when they started, how far they have progressed, what type of transformations are brought to the environment through these actions, and what people will do next. It also enables diverse downstream applications, such as video security or surveillance systems, assistive technologies, and human-robot interactions. This survey first introduces the techniques required to understand the task followed by a comprehensive overview of recent temporal action segmentation methods.

In computer vision, *action recognition* is the hallmark task for video understanding. In action recognition, pre-trimmed video clips of a few seconds are classified with single semantic labels. State-of-the-art methods [2], [3], [4], [5], [5] can distinguish hundreds of different classes [6], [7]. However, classifying pre-trimmed clips is a highly limiting case as the video feeds of surveillance systems, autonomous vehicles, and other real-world systems occur in streams. The individual actions or events are related and may span

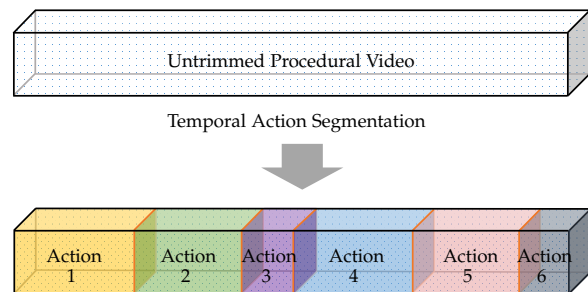


Fig. 1: Temporal Action Segmentation segments an untrimmed video sequence in the temporal dimension into successive actions.

well beyond a few seconds. As a result, standard action recognition approaches are not directly applicable.

In contrast with the pre-trimmed clips of action recognition, temporal action segmentation methods target untrimmed video sequences. The videos depict a sequence of multiple actions, often spanning several minutes. Typically, the videos show a procedural activity. Fig. 2 shows a 4-minutes-long video posted on YouTube of “making coffee”¹ with six steps: ‘add ground coffee’, ‘add sugar’, ‘add water’, ‘mix coffee’, ‘add milk’ and ‘add mixture’. In the procedural video domain, the prevailing terminology for the overall procedure is *(complex) activity*, while the composing steps are *actions*. Notably, the actions often follow a loose temporal ordering, *i.e.*, permutations of some actions in time, or the absence of certain actions still achieves the goal.

Temporal action segmentation is closely related to key-frame detection [8], [9] and temporal action localization [10],

- Guodong Ding and Angela Yao are with the School of Computing, National University of Singapore, Singapore (emails: dinggd@comp.nus.edu.sg, ayao@comp.nus.edu.sg).
- Fadime Sener is a research scientist at Meta Reality Labs (email: fame-sener@meta.com).
- * indicates equal contribution.

Manuscript received October 19, 2022

1. <https://www.youtube.com/watch?v=9hTai5mb1jg>



Fig. 2: An illustrative video of “making coffee” that features in total six steps. “Making coffee” is the *procedural activity*, while the numbered steps are ‘actions’. The actions performing an activity may follow a loose ordering with some actions sequentially interchangeable, e.g., ‘add sugar’ and ‘add water’.

[11]. Two factors distinguish the segmentation task: the first is the emphasis on the temporal boundaries and the second is the strong temporal relationships between actions that may span over the range of several minutes. Key-frame detection, as the name suggests, finds single representative frames of the actions, and is not concerned with identifying the start or end of actions or their duration. Temporal action localization has a detection focus and less dependence on the action orderings within the sequence.

Accounting for these distinguishing factor requires two considerations: discriminative frame-level representations and long-range temporal modelling. Frame-level representations should not only capture static but also dynamic discriminative visual cues. At a higher level, the actions are related to each other through sequence dynamics. The ordering characteristics of actions raises a fundamental question - how should temporal or sequential relationships be modeled to account for repetitive actions, variation in action duration and order? Accordingly, this survey considers the above two facets as the core techniques in temporal action segmentation tasks and provides detailed reviews, respectively.

Contributions: There are several surveys on human activity understanding in videos, though their focus is primarily on action recognition [12], [13], [14], [15], temporal action localization [16], [17], action anticipation [15], [18], [19], etc. To the best of our knowledge, this work is the first to offer a comprehensive review of temporal action segmentation works. Beyond grouping together existing works, we present a taxonomy to highlight their contributions. Additionally, we compare the existing datasets by analyzing their characteristics. In doing so, we present two metrics, *i.e.*, repetition and order variation scores, which characterize the temporal dynamics of actions and reveal that majority of these datasets are limited in action repetition and order variation. Finally, we differentiate between vari-

ous performance evaluation and comparison settings. We propose a standardized evaluation setup for unsupervised segmentation methods, as well as, a class based evaluation to emphasize the long-tail distribution. Lastly, we provide a few promising future directions and challenges for the community to explore.

1.1 Survey Structure

Fig. 3 outlines a taxonomy of the temporal action segmentation task and the structure of this survey. Section 2 provides a formal task description for temporal action segmentation and compares it with other related tasks. Section 3 presents the standard benchmarks adopted by the action segmentation community together with a detailed analysis on their temporal dynamics. Section 4 outlines the forms of supervisory signals used in existing works, evaluation metrics, and performance comparison settings. Section 5 delves into how frames are embedded and embellished, summarizing the widespread usage of handcrafted models or deep learning backbones for feature extraction. Section 6 outlines the temporal and sequential modeling techniques employed in temporal action segmentation. Sections 7 to 10 provides a comprehensively curated list of temporal action segmentation approaches grouped according to the type of supervision. Finally, Section 11 concludes the survey by discussing challenges and future research directions.

2 TEMPORAL ACTION SEGMENTATION

2.1 Task Description

Temporal action segmentation aims to segment a temporally untrimmed video by time and label each segmented part with a pre-defined action label [20]. Formally, given a video $x = (x_1, x_2, \dots, x_T)$ of length T with N actions, temporal action segmentation methods produce the following output:

$$s_{1:N} = (s_1, s_2, \dots, s_N) \tag{1}$$

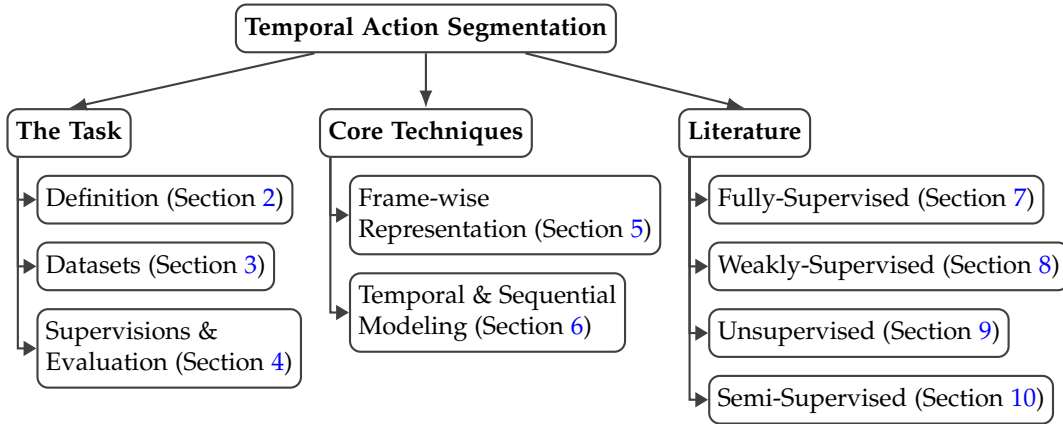


Fig. 3: The taxonomy of existing temporal action segmentation research.

where $s_n = (c_n, \ell_n)$ represents a continuous video segment of length ℓ_n that has the semantic label c_n out of \mathcal{C} predefined categories. The task can also be regarded as a 1D version of semantic (image) segmentation, and can analogously be formulated as a frame-wise action classification, *i.e.*,

$$y_{1:T} = (y_1, y_2, \dots, y_T) \quad (2)$$

where y_t is the action label of frame t . The segment formulation is commonly used in works that predict the most probable sequence of actions [21], [22], while the latter, frame-wise formulation is popular with deep learning-based methods [23]. The two formulations, however, are equivalent and one can easily reconstruct one from the other.

2.2 Related Tasks

There are several tasks in video understanding which are closely related to temporal action segmentation (TAS). They can be distinguished with action segmentation based on their data domain, identification of segment semantics as well as the reasoning of temporal dynamics between segments [10], [24], [25]. The related tasks are described below and compared in Tab. 1.

Temporal Action Detection / Localization (TAD/L) [10], [11], [26], [27] detects the start and end timestamps of action instances and finds the corresponding semantic labels simultaneously. TAD/L is a temporal detection task; together with TAS, the two are the 1D analogues of object detection and semantic segmentation. TAD/L allows overlap in the actions, while TAS finds a transition point between actions. Unlike TAS, which works mostly with procedural sequences, TAD/L works more with general videos that do not feature such strong temporal relations between actions. Commonly used datasets in TAD/L are THUMOS14 [28] and ActivityNet [29], which feature sport activities and/or everyday activities such as ‘walking a dog’. As a result, the localized actions are sparse in time.

Sequence Segmentation Tasks (SS) is popular on other domains including parsing motion capture data [24], [30], [31], [32] and dividing audio signals into small segments [33]. Most approaches are developed for segmenting individual sequences [30], [31], [32] while several [34] focused on segmenting multiple motion capture recordings

simultaneously. However, such data is lower-dimensional and exhibits much less variance than video, making it difficult to transfer these methods directly to the video data without strong appearance models.

Key-Frame Detection (KFD) identifies single characteristic frames or key-steps [8], [9], [25], [35], [36], [37], [38] for actions. One line of work [25], [35] targets finding the key-frames from a collection of narrated videos with weak supervision from the narrations. Another line of work [36], [38] is based on subset selection, which is frequently used in document summarization, and aims to discover a small subset of the most informative data points. KFD is also investigated under fully-unsupervised settings [8] where no text data is used and under semi-supervised settings [39]. Like TAS, KFD requires modeling the temporal relations between actions; however, it does not need to find the boundary where the actions transition.

Complex Activity Classification (CAC) targets classifying the complex activity of procedural videos. Methods typically utilize temporal convolutions [40], [41], gating mechanism for sampling representative segments [42] and graphs for representing complex activities [43]. Such methods are similar to TAS in the way they model the temporal relations of actions, but they are not concerned with the individual frames as their aim is to determine the complex activity class of the entire action sequence.

Generic Event Boundary Detection (GEBD) [44] aims to localize the moments where humans naturally perceive event boundaries. The boundaries signify changes in action, subject, and environment. In comparison, GEBD does not involve any predefined semantic classes as targets and does not assume any temporal relations between detected boundaries.

3 DATASETS

3.1 Core Datasets

Datasets used for evaluating temporal action segmentation methods usually feature procedural activity videos [25], [45], [46], [47], [48]. Actors execute a sequence of actions, following some order, to arrive at a goal, such as making a dish, or assembling some furniture. Such datasets are typically annotated with action segments’ start and end boundaries and action labels.

TABLE 1: Comparing Temporal action segmentation with related tasks in four aspects, differentiating the tasks based on whether they involve Temporal Relation between action instances in videos, Boundary Localization of actions, Segment Semantic understanding of actions, and the Data Domain. As it is shown, temporal action segmentation has its own unique position in the task landscape.

Task	Temporal Relation	Boundary Localization	Segment Semantic	Data Domain
TAD/L	✗	✓	✓	video
SS	✓	✓	✓	audio, motion
KFD	✓	✗	✓	video, text
CAC	✓	✗	✗	video
GEBD	✗	✓	✗	video
TAS	✓	✓	✓	video

Four datasets used in temporal action segmentation works are GTEA [45], 50Salads [46], Breakfast Actions [47], or YouTube Instructional Videos [25]. Most recently, Sener *et al.* [48] presented Assembly101, with coarse action segment labels targeted towards temporal action segmentation. Of these datasets, Breakfast Actions, GTEA, and 50Salads are kitchen activities. YouTube Procedural [25] is a curated collection of YouTube videos of instructional activities. Assembly101 [48] includes recordings where people disassemble and assemble toys that can be taken apart.

- **GTEA** [45] contains 28 videos of seven procedural activities recorded in a single kitchen. The videos are recorded with a camera mounted on a cap worn by four participants.
- **50Salads** [46] is composed of 50 recorded videos of 25 participants making two different mixed salads. The videos are captured by a camera with a top-down view onto the work surface. The participants are provided with recipe steps, which are randomly sampled from a statistical recipe model.
- **Breakfast Actions** [47] targets recording videos “in the wild”, in 18 different kitchens, as opposed to the controlled lab environments in the previous datasets [45], [46]. The participants are not given any scripts, and the recordings are unrehearsed and undirected. The dataset features 52 participants performing ten breakfast-related activities and is recorded with 3 to 5 cameras, all from the third-person point of view.
- **YouTube Instructional** [25] is a collected dataset and includes five instructional activities. There are 30 videos for each activity. This dataset is mainly used for unsupervised segmentation.
- **Assembly101** [48] is a recently collected dataset where 53 participants are asked to disassemble and assemble take-apart toys without being given any instructions, resulting in realistic sequences with great variation in action ordering. The dataset is annotated with fine-grained, hand-object interactions and coarse action labels, which are composed of multiple fine-grained action segments related to the attaching or detaching of a vehicle part. The authors evaluate their dataset for temporal action segmentation using coarse labels.

3.2 Related Datasets

There are several other long-range procedural activity datasets. In this section, we present these datasets and explain why it is challenging or not preferable to explore temporal segmentation on these datasets.

- **YouCookII** [49] is collected from YouTube. Each video, all from cooking recipes, is annotated with the temporal boundaries of the recipe steps and their textual description but no action labels to be used in the temporal action segmentation works.
- **COIN** [50] is a large-scale dataset collected from YouTube that includes a diverse number of 180 different tasks from these twelve domains. However, the videos are composed of, on average, four segments, making studying the sequence dynamics less interesting.
- **Meccano** [51] is a recently recorded dataset in which 20 people are assembling a toy motorbike. It only includes fine-grained action labels.
- **Ikea ASM** [52] includes videos of the assembly of four IKEA furniture types and is annotated with fine-grained actions only.
- **CrossTask** [35] It is collected from YouTube and includes two types of tasks: 18 primary tasks that are fully annotated with the actions’ temporal locations and 65 related tasks without any temporal annotations, collected to complement the primary tasks. Although some unsupervised segmentation methods [53] are benchmarked on this dataset, CrossTask is not commonly used for evaluating supervised or weakly supervised methods.
- **Epic-Kitchens** [54], [55] is a large-scale egocentric dataset with 100 hours of recording. The duration of videos ranges from 1 to 55 minutes. Although it includes long-range videos, it might not be very suitable for segmentation as it includes overlapping segments and contains only fine-grained action labels.

3.3 Dataset Comparison & Discussion

Tab. 2 makes a detailed comparison of the procedural video datasets. The datasets can be divided according to their data source, scale, number of actions, viewpoint, either being dedicated recordings [45], [47], [56] or curated from online video platforms like YouTube [49], [50].

Recorded datasets have either third-person or egocentric views. Datasets with third-person view only contain constrained backgrounds and are more focused on foreground action. However, they may suffer from the occlusions of actions due to the fixed view of cameras. While the egocentric view is better at capturing objects, tools to recognize the hand object interactions, the camera motion correctly poses extra challenges to action recognition.

The Epic-Kitchens dataset [55] is the largest dataset in egocentric vision that captures untrimmed daily activities. There are also several procedural activity datasets with an egocentric view, *e.g.*, [45], [56], but on a much smaller scale. The Breakfast Actions dataset [47] contains multi-view recordings. However, all the views are from a third-

TABLE 2: Comparisons of procedural activity datasets in a chronological order. The first group of datasets are Recorded while the second group of datasets are from Online media platforms, *e.g.*, YouTube. We report the Duration, the number of videos (# Videos), segments (# Segments), procedural activities (# Activity), actions (# Action) and Domain for each dataset. The View of datasets might be Egocentric, 3rd Person, Top-view, or Mixed.

	Dataset	Year	Duration	# Videos	# Segments	# Activity	# Action	Domain	View
Recorded	[45] GTEA	2011	0.4h	28	0.5K	7	71	Cooking	Egocentric
	[46] 50Salads	2013	5.5h	50	0.9K	1	17	Cooking	Top-view
	[47] Breakfast	2014	77h	1712	11K	10	48	Cooking	3rd Person
	[55] Epic-Kitchens	2020	200h	700	90K	-	4053	Daily	Egocentric
	[52] Ikea ASM	2021	35h	371	16K	4	33	Furniture	3rd Person
	[51] Meccano	2021	0.3h	20	8.9K	1	61	Assembly	Egocentric
	[48] Assembly101	2022	513h	4321	1M	15	202	Assembly	Egocentric + 3rd Person
Online	[25] YouTube Instructional	2016	7h	150	-	5	47	Mixed	Mixed
	[49] YouCookII	2018	176h	2K	15K	89	-	Cooking	Mixed
	[35] CrossTask	2019	376h	4.7K	34K	83	107	Mixed	Mixed
	[50] COIN	2019	476h	11.8K	46K	180	778	Mixed	Mixed

person perspective. Only Assembly101 [48] provides both egocentric and third-person views.

Sourcing videos from online platforms is a convenient way to build up large-scale and varied datasets [35], [49], [50], [57], [58]. Although these datasets may be useful for training offline retrieval systems, they may not be applicable to real-time scenarios such as action anticipation and augmented reality-related tasks, as online videos are edited, *e.g.*, with fast-forwarding, annotated frames or changing viewpoints. Assembly101 is the largest recorded procedural activity dataset, while COIN is the largest collected one.

Procedural activity understanding is a very promising topic due to the increasing amount of “how-to” videos. Moreover, it can have a big impact on real-time smart systems assisting with various tasks. However, the diversity in the existing activity datasets is rather limited. Although the collected datasets recently started including diverse domains [50], almost all the recorded datasets, with a few recent exceptions [51], [52], cover only cooking activities. These new datasets, on the other hand, are too small. As of the moment, Assembly101 [48] is the only dataset that offers a large-scale data which is beyond the kitchen domain.

3.4 Background Frames

Depending on the source of the procedural video, there may be segments in a sequence irrelevant to task completion. For example, the actor may talk or give recommendations without performing any action of interest or introduce tools or alternative ways to complete the step, etc. Depending on how the video is made, such segments can occur arbitrarily and vary in duration. Such ‘background frames’ can be found in datasets collected from YouTube, such as YouTube Instructional [25], YouCookII [49], and CrossTask [35] at varying degrees *e.g.*, 73% in [25] or see Fig. 4 for GTEA.

In most existing temporal action segmentation works, the background class is considered as an equivalent to other action classes and is directly used for training and evaluation.

3.5 Temporal Dynamics

A defining characteristic of the temporal action segmentation task is the sequence relationships between the actions. To better understand and characterize the sequence dynamics, we propose two scores, repetition score and order

TABLE 3: Temporal dynamics of coarse action segments. A higher value in **Repetition** score indicates more action repetition, while a lower value in **Order Variation** score indicates looser action ordering constraints.

Dataset	Repetition $r \uparrow$	Order Variation $v \downarrow$	IR
[46] 50Salads	0.08	0.02	6
[47] Breakfast	0.11	0.15	639
[48] Assembly101	0.18	0.05	2604

variation, and compare the scores of the core datasets in Tab. 3.

We define the **repetition score** r to reflect the portion of repetitive ones amongst all actions, which is formulated as,

$$r = 1 - u/g \tag{3}$$

where u is the number of unique actions in one video instance, and g is the total number of actions, and r is a score falls in the range of $[0, 1)$. 0 indicates no repetition, and the closer the score is to 1, the more repetition occurs in the sequence.

The **order variation score** v is defined as the normalized average edit distance, $e(R, G)$, between every pair of sequences, (R, G) . It is then normalized with respect to the maximum sequence length of the two,

$$v = 1 - e(R, G)/\max(|R|, |G|) \tag{4}$$

This score has a range $[0, 1]$; a score of 1 corresponds to no deviations in ordering between pairs. A high score indicates that actions follow a strict ordering, making it less necessary to model temporal sequence dynamics. On the other hand, a very low score, like in 50Salads, indicate the highest amount of ordering variations as salad items can be added at any time, making modelling the temporal relations between actions less beneficial.

Compared to existing datasets, Assembly101 positions itself as a challenging and interacting benchmark for modelling the temporal relations between actions. As indicated in Tab. 3, compared with Breakfast and 50Salads, Assembly101 includes $1.6\times$ and $2.3\times$ more repeated steps, respectively. Assembly101’s higher order variations score than Breakfast and lower order variation score than 50Salads makes it more relevant to model temporal relations between actions.

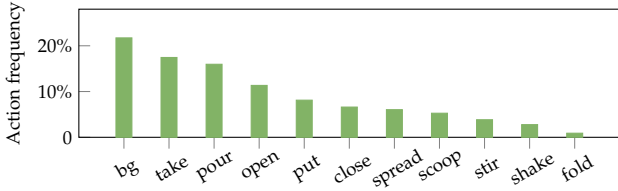


Fig. 4: Action frequency on GTEA [45], sorted by a descending order. ‘bg’ indicates the ‘background’ where no action of interest occurs. The head class ‘bg’ is 24× more frequent than the tail class ‘fold’.

TABLE 4: Imbalance Ratio (IR) on four TAS datasets. A higher IR value indicates the

Dataset	GTEA	50Salads	Breakfast	Assembly101
IR	24	6	639	2604

3.6 Action Frequency

The long-tailed action frequency is an overlooked aspect of per-frame classification formulation (Eq. (2)) of TAS. In procedural videos, it is natural that some actions require a longer time to perform than others, *e.g.*, ‘fry egg’ is considerably more time-consuming than ‘crack egg’. We calculate the action frequency as the proportion each action label takes in the whole dataset, *i.e.*, $n_c / \sum_{i=1}^C n_i$, where n_c is the number of frames with label c . Fig. 4 illustrates the action frequency on the GTEA dataset [45], which depicts the imbalanced frequencies across actions.

A commonly adopted value to indicate the skewness of the action frequency is the imbalance ratio (IR) [59], [60]. IR is defined as the ratio between the number of frames in the head and the tail classes (n_1/n_K) sorted by the decreasing order of cardinality (*i.e.*, if $i_1 > i_2$, then $n_{i_1} \geq n_{i_2}$ and $n_1 \gg n_K$). Tab. 4 shows that 50Salads [46] has the smallest IR value of 6, marking a less imbalanced scenario between actions; however, Assembly101 [48] is highly skewed in action frequencies with a IR of 2604. Such a long-tailed nature of the datasets poses extra challenges to the temporal action segmentation task. However, little effort has been dedicated to explore and investigate this inherent problem in procedural activities.

4 SUPERVISION AND EVALUATION

4.1 Task Supervision

Like many other computer vision tasks, temporal action segmentation has been investigated under different forms of task supervision. Tab. 5 lists the forms of supervision in descending order in terms of annotation effort, *i.e.*, from fully-supervised to unsupervised.

A fully-supervised setting provides dense action labels for every frame in training video sequences [23], [61]. Dense labels are the most time-consuming to collect per video sequence as it requires the annotator to view the entire video sequence. A semi-supervised [62], [63] setting reduces the annotation effort proportionally by annotating a subset of the videos densely while treating the remaining videos as unlabeled samples.

Weakly labels require less annotation efforts than dense video labels. Weak labels explored in the literature include

single-frames [64], [65], action lists or action sets [21], [22], and activity labels [66]. Single-frames, or time-stamp annotations, are sparsely labelled frames, and can be viewed as an ordered list of actions associated with exemplar frames. Removal of the exemplar frames would form the supervision dubbed as action list, which has the exact same level of supervision as action transcript. Further reducing the ordering of actions, and repetitive entries from action list leads to a even weaker supervision, categorized as an action set.

The above-listed weak forms of supervision variants are all based on the action-level annotations. Recently, Ding *et al.* [66] proposed adopting video-level complex activity labels to supervise the action segmentation task. Due to the absence of any action level information, activity label supervision is the weakest form of annotation.

The unsupervised setting in temporal action segmentation in previous works [67], [68], [69] considers collections of videos that perform the *same* activity. In this regard, it is not label-free, as it requires the activity label to form the video collections. The unsupervised setting then is comparable with the weak activity label supervision in terms of label information. However, the two settings differ in how the collections of videos are processed during training. Formally, unsupervised works work with one group of the same activity videos at a time, while activity label supervision works with videos from all activities simultaneously.

4.2 Evaluation Measures

Three commonly adopted evaluation metrics in action segmentation are Mean of Frames (MoF), Edit Score and F1-scores. The first is a frame-based measure (see Section 4.2.1), while the latter two are segment-based measures (see Section 4.2.2). All three metrics are used in fully, weakly and semi-supervised settings. For unsupervised settings, only F1 and MoF are more reported in the literature. By definition, the evaluation the unsupervised works is conditioned on the association between clusters and semantic labels. The Hungarian matching algorithm has been adopted to enable the evaluation by mapping learned frame clusters to semantic labels, which we elaborate in detail in Section 4.4.

4.2.1 Frame-Based Measures

Frame-wise accuracy (Acc), also referred to as Mean over Frames (MoF), is defined as the fraction of the model’s correctly predicted frames:

$$\text{Acc} = \frac{\# \text{ of correct frames}}{\# \text{ of all frames}}. \tag{5}$$

The Acc metric is problematic when the action frame distribution is imbalanced. This is true for most datasets, as dominating (long) actions class can have a strong impact on the value. The existence of such imbalance as we have discussed in Section 3.6 makes this more likely to happen. This also implies that models achieving similar accuracy may have large qualitative differences. Therefore, a class averaged accuracy metric would help better interpret the model performance, *e.g.*,

$$\text{mAcc} = \frac{\sum_c \text{Acc}(c)}{|C|} \tag{6}$$

TABLE 5: Comparison of supervisory signals and evaluation prerequisites in temporal action segmentation. Full supervision provides frame-wise dense action labels. The single-frame under weak supervision setting provides an ordered list of actions per video with corresponding exemplar frames. Evaluation of such two settings relies on the network predictions without any pre-steps. Action lists or set supervision do not provide exemplars. Evaluation under this setting is based on the best-matched action list searched with maximum sequence posterior for each test video. Activity label setting uses the same amount of supervision information as the unsupervised counterpart. However, ours uses all complex activity videos simultaneously, unlike unsupervised ones, which use them one at a time. Since no action-level signals are provided, it is necessary to perform Hungarian matching before evaluation.

	Full (Section 7)	Semi (Section 10)	Weak (Section 8)			Unsupervised (Section 9)
			Single-frame	Action List/Set	Activity Label	
Action-level	Dense frame-wise	subset with Dense frame-wise	Ordered list + Exemplar frames	(Ordered) list, Union set	-	-
Video-level	-	-	-	-	All activities <i>en masse</i>	One activity at a time
Evaluation prerequisite	-	-	-	Maximum Sequence Posterior (Section 4.3)	Hungarian Matching (Section 4.4)	Hungarian Matching (Section 4.4)

where $\text{Acc}(c)$ is the frame accuracy per class c .

Another drawback of MoF is that its per-frame calculation can not reflect the segmental quality. The MoF score could be high even when the segmentation results are fragmented. Such division of a durative action into many discontinuous sub-segments is referred as over-segmentation. However, over-segmentation can be evaluated by segment-based measures, as introduced next.

4.2.2 Segment-Based Measures

The segment-based F1-score [61] and Edit Score [70] are evaluation metrics that more focus on the segment errors.

The F1-score, or $\text{F1@}\tau$ [61] compares the Intersection over Union (IoU) of each segment with respect to the corresponding ground truth based on some threshold $\tau/100$. A segment is considered a true positive if its score with respect to the ground truth exceeds the threshold. If there is more than one correct segment within the span of a single ground truth action, then only one is considered a true positive and the others are marked as false positives. Based on the true and false positives as well as false negatives (missed segments), one can compute the precision and recall and blend the two into the a harmonic mean to get

$$\text{F1} = 2 \cdot \frac{\text{precision} * \text{recall}}{\text{precision} + \text{recall}}. \quad (7)$$

Normally, τ values are set to $\{10, 25, 50\}$.

The Edit Score [70] quantifies the similarity of two sequences. It is based on the Levenshtein distance, tallies the minimum number of insertions, deletions and replacement operations required to convert one segment sequence into another. By denoting by X and Y the ordered list of predicted and ground truth action segments, the accumulative distance value e is defined as:

$$e[i, j] = \begin{cases} 0, & i = 0, j = 0 \\ j, & i = 0, j > 0 \\ i, & i > 0, j = 0 \\ \min(e[i - 1, j] + 1, & \\ e[i, j - 1] + 1, & \\ e[i - 1, j - 1] + 1, & \\ \mathbb{1}(X[i] = Y[j])), & i > 0, j > 0 \end{cases}, \quad (8)$$

where $i \in |X|, j \in |Y|$ are indices for X and Y , respectively, and $\mathbb{1}(\cdot)$ is the indicator function. The above problem can

be effectively solved by dynamic programming. The Edit Score is then normalized by the maximum length of the two sequences and is computed as:

$$\text{Edit} = \frac{1 - e(X, Y)}{\max(|X|, |Y|)} \cdot 100. \quad (9)$$

This metric measures how well a model predicts the action segment ordering without requiring exact frame-wise correspondence to the ground truth.

The methods working with full-supervision, semi-supervision and single-frame weak-supervision can evaluate the task performances directly with the above evaluation procedure and do not require any pre-requisitions. Given a segmentation model that predicts frame-wise action probability scores, the performance is directly evaluated by taking frame-wise predictions and comparing with their corresponding ground truth labels to compute the three scores defined above.

4.3 Weakly-Supervised Evaluation

For the model inference on the test set where no reference action list or set is available, Richard *et. al.* [22] presumes that the set of actions appearing in a test video overlaps with that from the training set, *i.e.*, there is at least one training video sharing the same ground truth action set as the test video. Similarly, Li and Todorovic [71] follow [22] and use the same Monte Carlo sampling of potential actions sequences, but discard candidate sequences that do not include all actions in that video. Out of all K sampled candidates, the action sequence that gives the maximum posterior modeled by a Hidden Markov Model (HMM) Eq. (19) is selected as the final solution. A detailed description of the posterior estimation is provided in Section 6.2.1.

4.4 Unsupervised Evaluation

The evaluation measures in Section 4.2 are not directly applicable to the unsupervised setting without some correspondence between the estimated agnostic segments and ground truth action classes. The Hungarian matching algorithm [72] is a combinatorial algorithm that can be used to find maximum-weight matching in bipartite graphs, and it has been widely used for evaluating unsupervised clustering tasks [73], [74].

In unsupervised temporal action segmentation, given a predicted frame-wise label corpus X of N clusters and the

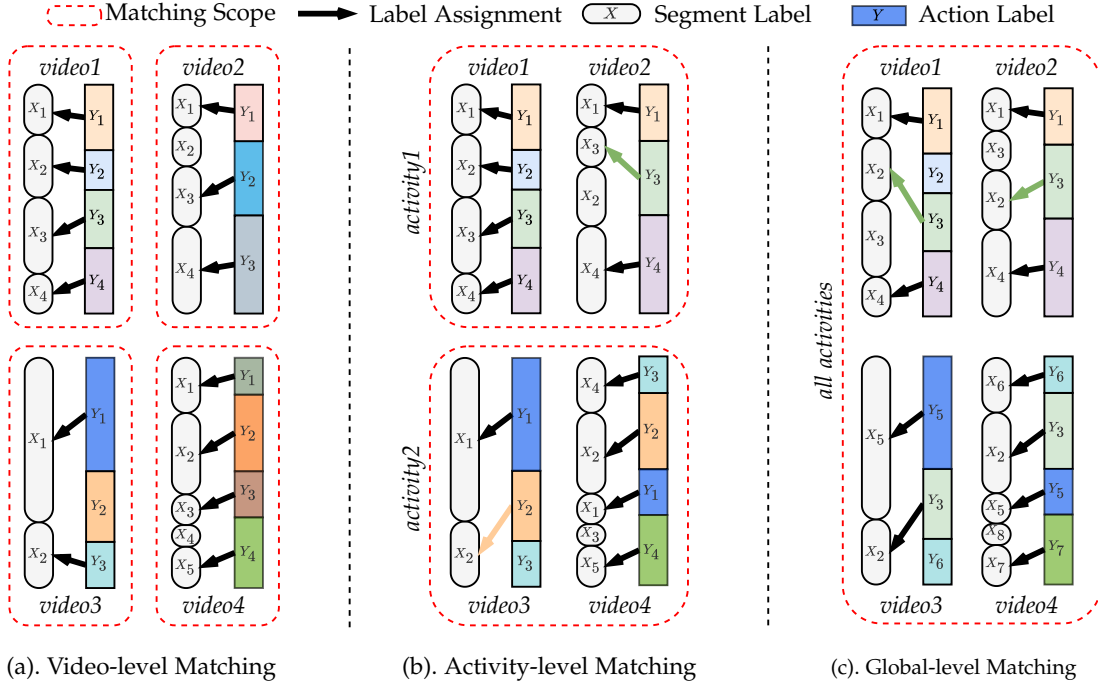


Fig. 5: Label assignment illustration of four videos from two complex activities under different levels of Hungarian matching. Rounded rectangles denote video segment labels, and colored rectangles denote ground truth action labels. The red dashed rectangles denote the scopes of Hungarian matching. The black dashed arrows denote matched segments while the coloured arrows highlight differences in actions as matching scope changes. As the scope changes from the video-level (a) to the activity-level (b), ground truth action labels Y for different videos first relate themselves according to their semantic meaning, and therefore result in the change of label assignment for *video2* (green) and *video3* (orange). A similar change of assignments happens when the matching is done on the global level (c). Unmatched segments (X_2 in *video2* at video-level matching (a)) in practice are considered as background.

entire ground truth action label corpus Y of M semantic classes, Hungarian matching relates N clusters to M semantic labels by finding the best matching $\hat{\mathcal{A}} \subset \{0, 1\}^{N \times M}$ defined as:

$$\hat{\mathcal{A}} = \arg \max_{\mathcal{A}} \sum_{n,m} \mathcal{A}_{n,m} \cdot I(X_n, Y_m), \quad (10)$$

s.t. $|\mathcal{A}| = \min(N, M)$

where X_n denotes frames belonging to cluster n , and Y_m denotes frames with the action label m . $\mathcal{A}_{n,m}$ is the indicator function for assigned pair (n, m) , $I(X_n, Y_m)$ is the number of frames with ground-truth class label m that appear in cluster n .

The Hungarian matching forms a bijection when two parties have equal classes ($N = M$). Otherwise, it results in a one-sided-perfect matching with the matching size of $\min(N, M)$. In practice, the remaining unmatched frame clusters are automatically considered as the background when $N > M$. After matching, the results are then computed by the frame-based measure as introduced in Section 4.2.1.

Matching Scope Depending on the bipartite set's scope (X and Y), Hungarian matching can be applied at the *video-level*, *activity-level*, and *global-level*, as illustrated in Fig. 5.

Video-level matching [68], [75] matches the labeled actions with respect to the ground truth actions of a *single* video. This level of matching evaluates the ability of a method to partition a video sequence into the individual actions. Because matching is done at the video level, the segmentation method does not need to associate actions across videos

TABLE 6: Comparison between model learning requirements in different levels of Hungarian matching for action segmentation. For **video-level** matching, Intra-Video Discrimination of actions is sufficient. To enable an **activity-level** matching, the model needs to take into consideration Intra-Activity Association. Meanwhile, the **global-level** matching sets the highest learning requirement with additional Inter-Activity Association between actions.

Matching Level	Intra-Video Discrimination	Inter-Activity Association	Inter-Activity Association
Video	✓	✗	✗
Activity	✓	✓	✗
Global	✓	✓	✓

and produces the best performance of the three scopes. In Fig. 5(a), within each matching scope, the Hungarian matching is performed per video and is agnostic of the possible association of actions across videos.

Activity-level matching associates clusters and action labels within each complex activity. Most unsupervised works [67], [76], [77] follow this level of matching, *i.e.*, process each complex activity individually. As shown in Fig. 5(b), the activity level of grouping has led to the assignment changes denoted by colored arrows.

Lastly, *global-level* matching is based on the output prediction and ground truth of all video frames on the entire dataset. This is the most challenging setting as both intra- and inter-activity matching must be considered. It is noteworthy that [76] report a different 'global' matching results

across complex activities, as their setting does not consider actions shared across complex activities.

The various scopes of Hungarian matching corresponds to different modelling aims; the broader the scope, the more challenging the task. Video-level matching only requires disambiguating actions within a single video, *i.e.* *intra-video action discrimination*. For activity-level matching, a model must discriminate between actions within a video and also learn *intra-activity action association*. The broadest global-level matching requires a model to also incorporate *inter-activity associations* to establish feasible action correspondences across the complex activities. The differences in these learning requirements for the three matching scopes are summarized in Tab. 6. Note that a model learned at a broader scope is **downward compatible** and can be adjusted to be evaluated at a finer scope, *e.g.* from global to activity level, but not vice-versa. Despite the practical feasibility of doing so, the results are not directly comparable because of their divergent learning requirements.

5 FRAME-WISE REPRESENTATION

In deep learning, feature representations can be either learned end-to-end with respect to the task or pre-learned independently. The standard practice in action segmentation is to use pre-computed frame-wise features (Section 5.1) as inputs, due to the heavy computational demands of learning video features. Using pre-computed features has a key advantage in that it allows a dedicated comparison of the proposed architectures without the confounding influences of improved frame-wise feature representations. More recently, some works have aimed making the pre-computed features more discriminative (Section 5.2) by embedding more task-specific knowledge.

5.1 Pre-Computed Features

5.1.1 Fisher Vector Encoded IDT

The original and Improved Dense Trajectories (IDT) [78], [79] were commonly used hand-crafted features for action recognition and video understanding before the rise of deep learning. The original dense trajectories features [78] are spatio-temporal features computed along tracks of interest points formed via optical flow. IDT [79] adds “improvements” by correcting the trajectories for camera motions. To apply IDT to action recognition, [79] further encode the raw trajectories by using Fisher Vectors (FV) [80] to capture the trajectories’ first and second order statistics.

Fisher vectors are characterized by a gradient vector derived from a generative probabilistic model. Given a D -dimensional feature set $\mathbf{F} = \{f_t : t = 1, \dots, T\} \in \mathbb{R}^{D \times T}$ extracted from a video clip of length T , it is assumed that the generation process of \mathbf{F} can be modeled by a probability density function u_λ with the parameter λ [80]. In video understanding, this density is often modeled as a K component Gaussian Mixture Model, *i.e.*, $u_\lambda(f) = \sum_{i=1}^K w_i u_i(f)$ with the parameters $\lambda = \{w_i, \mu_i, \sigma_i : i = 1, \dots, K\}$, where

w_i , μ_i and σ_i denote the mixture weight, mean vector and variance² vector of Gaussian u_i respectively.

Thus, \mathbf{F} can be represented by the gradient vector [81]:

$$G_\lambda^{\mathbf{F}} = \frac{1}{T} \sum_{t=1}^T \nabla_\lambda \log u_\lambda(f_t) \quad (11)$$

In the Gaussian mixture, let the soft assignment $\gamma_t(i)$ of a given frame f_t to Gaussian u_i be:

$$\gamma_t(i) = \frac{w_i u_i(f_t)}{\sum_{j=1}^K w_j u_j(f_t)}. \quad (12)$$

The gradients with respect to each mean μ_i and variance σ_i can then be derived as:

$$\mathcal{G}_{\mu,i}^{\mathbf{F}} = \frac{1}{T \sqrt{w_i}} \sum_{t=1}^T \gamma_t(i) \left(\frac{f_t - \mu_i}{\sigma_i} \right), \quad \text{and} \quad (13)$$

$$\mathcal{G}_{\sigma,i}^{\mathbf{F}} = \frac{1}{T \sqrt{2w_i}} \sum_{t=1}^T \gamma_t(i) \left[\frac{(f_t - \mu_i)^2}{\sigma_i^2} - 1 \right]. \quad (14)$$

While one can also define an additional gradient with respect to the mixture weights w_i , this brings little added information [82], and so it is omitted in practice.

The gradients in Eq. (13) and Eq. (14) are concatenated over the K Gaussians to form a $2 \times D \times K$ dimensional FV representation of the original feature $G_\lambda^{\mathbf{F}} = [\mathcal{G}_\mu^{\mathbf{F}}, \mathcal{G}_\sigma^{\mathbf{F}}]'$. These vectors are then L_2 - and power-normalized [80] before applying dimensionality reduction. For temporal action segmentation models, the convention is to reduce the features from the original 426 dimensions to 64 via PCA [83].

5.1.2 Inflated 3D ConvNet (I3D)

Inflated 3D ConvNet (I3D) [2] is a state-of-the-art architecture to extract generic features for video understanding. It uses as a backbone the pre-trained Inception-V1 network [84] with 2D ConvNet inflation. In practice, it inflates all $N \times N$ spatial kernels to $N \times N \times N$ by replicating the original kernels N times and rescaling them with a temporal factor of $1/N$. Model parameters are trained on the Kinetics dataset [85] for action recognition. Architecture-wise, the I3D model has two data streams *i.e.*, RGB and optical flow. For feature extraction, the optical flow of the input video is computed by the TV-L1 algorithm [86]. Then, a $21 \times 224 \times 224$ spatio-temporal volume of RGB and flow frames are each fed into their respective networks to extract 1024D features. The two are then concatenated to obtain the final 2048D representation [87].

5.2 Additional Feature Learning

5.2.1 Discriminative Clustering

To cluster the video features discriminatively, Sener *et al.* [67] first learn a linear mapping Φ of the input features $\mathbf{X} \in \mathbb{R}^V$ into a latent embedding space, *i.e.*, $\Phi(\mathbf{X}) \in \mathbb{R}^E$. In the latent space, they define a set of K anchors $\mathbf{W}_a \in \mathbb{R}^{K \times E}$ to represent the potential action classes. The latent feature

² In practice, the covariance matrices are simplified to be diagonal, hence only variances are considered.

descriptor is then defined as a similarity with respect to the anchors, denoted as $\mathbf{F} = \mathbf{W}_a^T \mathbf{W}_\Phi \mathbf{X}$, where $\mathbf{W}_\Phi \in \mathbb{R}^{E \times V}$ are the embedding weights of Φ . The learning objective for the latent space is defined as a pair-wise ranking loss:

$$L = \sum_t \sum_{k=1, k \neq k^*}^K \max[0, f_t^k - f_t^{k^*} + \Delta] + \gamma \|\mathbf{W}_a, \mathbf{W}_\Phi\|_2^2, \quad (15)$$

where f_t^k denotes the distance of f_t to an anchor k and k^* is the action label for that video frame. The term $\Delta > 0$ is a predefined parameter which ensures that f_t is closer in the latent space to its anchor k^* than other anchors by a margin. L_2 regularization is imposed on \mathbf{W}_a and \mathbf{W}_Φ , and γ is the weighting parameter. In an unsupervised setting, as the true action label is unknown, \mathbf{W}_a and \mathbf{W}_Φ are learned iteratively, and k^* is assigned based on the segmentation results from a previous step.

5.2.2 Contrastive Learning

Contrastive learning builds robust feature representations by contrasting samples against each other to learn attributes that are common between data classes and attributes that set a data class apart from the others [88], [89], [90]. Inspired by these works, Singhania *et. al.* [62] applied contrastive learning to learn a set of stronger feature representations with a temporal encoder-decoder. The positive and negative sets of the contrastive learning are selected based on clustering and temporal continuity. K-Means is first applied on sub-sampled frames from the video corpus to output cluster labels for each frame, denoted as $l[f_i]$. Consider a given frame i in video n ; this frame's positive set $\mathcal{P}_{(n,i)}$ for contrastive learning will contain frame j from a different video m when both frames belong to the same cluster, *i.e.*, $l[f_i^n] = l[f_j^m]$, and are close by in time confined by a preset threshold δ , *i.e.*, $|t_i^n - t_j^m| < \delta$. This frame's negative set $\mathcal{N}_{(n,i)}$ is formed by candidate frame features that are in separate clusters, *i.e.*, $l[f_i^n] \neq l[f_j^m]$. The contrastive probability for a positive frame pair (i, j) from video (m, n) is then defined as:

$$p_{i,j}^{nm} = \frac{e_\tau(f_i^n, f_j^m)}{e_\tau(f_i^n, f_j^m) + \sum_{(r,q) \in \mathcal{N}_{(n,i)}} e_\tau(f_i^n, f_r^q)}, \quad (16)$$

where e_τ is the exponential cosine similarity with temperature τ .

The complex activity label can provide further cues for contrastive learning. In [62], video-level features h_n for video n are formed by max-pooling the frame features along the temporal dimension, *i.e.* $h_n = \max_{1 \leq t \leq T_n} f_{(n,t)}$. For video n with activity c_n , video-wise positive and negative sets can be constructed from other videos of the same or different activities, *i.e.*, $\mathcal{P}_n = \{m : c_m = c_n\}$ and $\mathcal{N}_n = \{m : c_m \neq c_n\}$ respectively. The contrastive probability for video n and its positive pair m is defined as:

$$p_{nm} = \frac{e_\tau(h_n, h_m)}{e_\tau(h_n, h_m) + \sum_{r \in \mathcal{N}_n} e_\tau(h_n, h_r)}. \quad (17)$$

Based on the frame- and video-level contrastive probabilities in Eq. (16) and Eq. (17), feature representations are

learned with following contrastive loss:

$$\mathcal{L} = -\frac{1}{N_1} \sum_{n,i} \sum_{m,j \in \mathcal{P}_{n,i}} \log p_{ij}^{nm} - \frac{1}{N_2} \sum_n \sum_{m \in \mathcal{P}_n} \log p_{nm}, \quad (18)$$

where $N_1 = \sum_{n,i} |\mathcal{P}_{n,i}|$ and $N_2 = \sum_n |\mathcal{P}_n|$.

5.2.3 Temporal and Visual Embedding

For highly regular activities like those found in Breakfast Actions, the same action tends to occur in a similar temporal range in the video sequence. Kukleva *et. al.* [76] leverage this fact and propose a pretext task of frame-wise timestamp prediction in a video to learn a temporal embedding. These temporal features are later used to find the potential temporal action clusters and their orders for subsequent action segmentation.

Vidalмата *et. al.* [77] later pointed out that a stand-alone temporal embedding lacks sufficient visual cues and proposed a two-stage pipeline to capture both visual and temporal representations of each frame. The first stage trains visual and temporal embedding models separately; a second stage trains both jointly. The visual embedding is learned with a frame prediction task to predict the feature at a future time $t + s$ based on feature input at current time t , while the temporal embedding model follows [76]. The second stage unites two models by imposing a frame reconstruction loss on the temporal model to predict frame representations that can give the best timestamp prediction.

Also based on the temporal embedding [76], Li *et. al.* [64] exploit the extra temporal relations on the action level by training a binary classifier on whether the input sequence of actions has been shuffled. Concretely, negative sequences are randomly sampled and shuffled while positive sequences remain in their original ordering. The final feature embedding is used for subsequent learning.

6 TEMPORAL AND SEQUENTIAL MODELING

Segmenting actions from the frame-wise features outlined in Section 5 typically requires some additional handling of dynamics or change over time. One approach captures the model directly into the network architecture, *i.e.* as part of a temporal convolutional network (TCN), a recurrent neural network (RNN) or a transformer. Others explicitly apply external models such as HMMs or Generalized Mallows Models. In accordance with the hierarchical structure of these videos, reasoning of the temporal dynamics can be categorized into frame level and segment level. We denote the frame-level model as temporal modeling and the segment-level model as sequential modeling.

6.1 Temporal Modeling

Temporal modeling on a frame-wise basis expands the temporal receptive field of the network and aggregates the dynamics in the feature representations. This level of modeling is necessary as commonly adopted pre-computed frame representations for temporal action segmentation were originally designed for action recognition on few-second-long video clips. Several works [91], [92], [93], [94] have shown that these features exhibit bias towards static cues, such as objects, scenes, and people. Efforts dedicated to

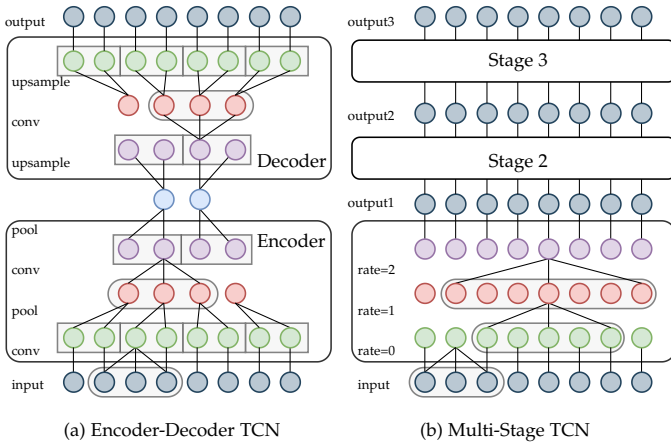


Fig. 6: Two exemplary types of Temporal Convolutional Networks (TCN) for temporal action segmentation. a) Encoder-decoder TCNs progressively enlarge the temporal receptive field via pooling. b) Multi-stage TCNs maintain a fixed temporal resolution with progressively larger dilated convolutions.

this problem include Recurrent Neural Networks, Temporal Convolutional Networks, and Transformers.

6.1.1 Recurrent Neural Networks (RNNs)

RNNs attempt to capture the temporal relations by encoding the complete sequence with the same set of shared parameters over time. Among them, Gated Recurrent Units (GRUs) [95] have been adopted in [96], [97]. Specifically, the GRU takes in frame inputs recurrently following their temporal order and predicts action labels. A similar GRU structure is used in [97] as the backbone, while they enable the bidirectional flow of the frames.

The memory of a frame-wise RNN stand-alone does not span long enough to capture the sequential relationship between actions. Above discussed methods [96], [97] are therefore usually combined with sequential modeling techniques which we introduce in Section 6.2. Another weakness of RNN is its limited ability in processing sequential inputs in parallel due to the recurrent dependencies between frames.

6.1.2 Temporal Convolutional Networks (TCNs)

Temporal Convolution Networks (TCNs) [61] use 1D convolutional filters in time. Two standard paradigms of TCNs, shown in Fig. 6, are encoder-decoders and multi-stage TCNs. Encoder-decoder TCNs [61], [98], [99], [100] shrink and then expand the temporal resolution with layer-wise pooling and upsampling in a U-Net fashion [101]. Alternatively, the multi-stage architecture (MS-TCN) expands the temporal receptive field with constant temporal resolutions via progressively larger dilated convolutions [23], [102]. Comparatively, the encoder-decoder architecture greatly reduces the computation time of long input sequences with temporal pooling which, however, may harm the prediction accuracy at action boundaries. On the contrary, the MS-TCN architecture preserves full resolution of frames, especially the boundary information at the cost of higher computation. The MS-TCN architecture generally produces better segmentation results than the encoder-decoder counterpart, making it the popular backbone network for many subsequent works.

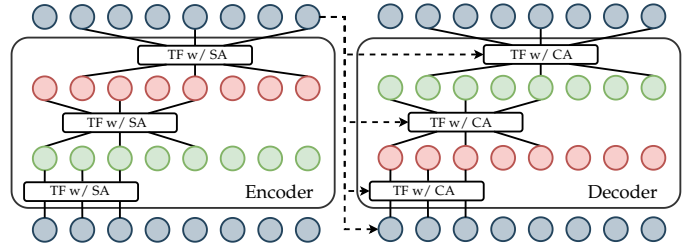


Fig. 7: Transformer architecture proposed for temporal action segmentation. The transformer blocks (TF) takes as input frames with increasing temporal dilation ratios d . The transformers in encoder uses self-attention (SA) across the frames. The decoder takes as input encoder outputs and uses cross-attention (CA) with them at each layer.

6.1.3 Transformer

Transformers, originally proposed for the machine translation problem in [103], have seen a quick adoption for videos [104], [105], [106], [107], [108], [109]. ASFormer [110] was the first work to explore the transformer architecture for the temporal action segmentation task. It adopts a similar encoder-decoder architecture as the ED-TCN [61] but replaces the convolutional operations with a transformer block receiving inputs with temporal dilations. In the encoder, the transformer only attends to frames within the inputs, which is often referred as self-attention (SA), while the blocks in the decoder adopt the cross-attention (CA) between features and the encoder outputs. An illustrative example is provided in Fig. 7. Building on top of ASFormer, Behrmann *et. al.* [111] adjusts the decoder part to only output the action sequence instead of frame-wise action labels, *i.e.*, mapping frame inputs to action sequence outputs.

The core technique of a transformer is its attention mechanism, which helps to aggregate the information. An earlier exploration with attention to temporal action segmentation was proposed by Sener *et. al.* [112]. They proposed a Temporal Aggregate Block (TAB) module which first utilizes non-local operation [113] to calculate the mutual attention between frames in multiple lengths of time span, and later fuses all spanning features with attentions via a Coupling Block. This type of temporal modeling is considered implicit as it is essentially building stronger feature representations based on neighbouring contexts. Although transformers are slowly being introduced for the temporal action segmentation task, the use is currently still limited. First, the transformers lack inductive biases, which would require a large corpus of videos to ensure effective training, but the existing datasets for temporal action segmentation are relatively small for large transformers to learn effective representations. Another problem indicated by [114] is that the self-attention mechanism may not learn meaningful weights from an extended span of inputs.

In summary, the temporal relationships for action recognition is modelled implicitly through the network architecture. Given the temporal convolution and attention operations discussed above, it is necessary for them to have access to the fine-grained frame-level annotation. Moreover, accurate action boundaries are of more importance to the model for learning ambiguities during action transitions.

6.2 Sequential Modeling

The actions in procedural videos typically follow some sequential order to serve a purpose or achieve a specific goal. Such sequential information is more easily captured on a segment level and various models such as Hidden Markov Models and Mallows Models have been investigated in the existing works [21], [67], [76].

6.2.1 Hidden Markov Model

Hidden Markov Models (HMMs) are a classic probabilistic models for working with sequential data input and they have also been applied to model the progression or sequential relations of action segments in video sequences. Recall that for a given video x , TAS is to find the optimal segments $\hat{s} = (\hat{c}, \hat{\ell})$, where $\hat{c} = [\hat{c}_1, \dots, \hat{c}_n, \dots, \hat{c}_{\hat{N}}]$ denotes the predicted ordering of action labels of length \hat{N} , $\hat{c}_n \in \mathcal{C}$, and $\hat{\ell} = [\hat{\ell}_1, \dots, \hat{\ell}_{\hat{N}}]$ are their corresponding temporal extents. The HMM to estimate the MAP $(\hat{c}, \hat{\ell})$ can be written as:

$$\begin{aligned}
 (\hat{N}, \hat{c}, \hat{\ell}) &= \arg \max_{N, c, \ell} p(c, \ell | x) & (19) \\
 &= \arg \max_{N, c, \ell} p(c) \cdot p(\ell | c) \cdot p(x | c, \ell) \\
 &= \arg \max_{N, c, \ell} p(c) \cdot p(\ell | c) \cdot p(x | c) \\
 &= \arg \max_{N, c, \ell} \underbrace{\left[\prod_{n=1}^{N-1} p(c_{n+1} | c_n) \right]}_{\text{context model}} \cdot \underbrace{\left[\prod_{n=1}^N p(\ell_n | c_n) \right]}_{\text{length model}} \\
 &\quad \cdot \underbrace{\left[\prod_{t=1}^T p(x_t | c_n) \right]}_{\text{visual model}}.
 \end{aligned}$$

The last term $p(x | c)$ in the third line is simplified from $p(x | c, \ell)$ since it is a frame-wise likelihood and does not depend on the action length ℓ .

The HMM formulation induces a model with three components. The first, $p(c)$, is a *context model*, providing probabilities for the sequence of actions in the video. As discussed in Section 5.2.3, CTE [76] assumes that similar actions tend to happen in close temporal vicinity so that the average timestamp $t(k)$ for feature clusters in the temporal embedding space is a good indication of the action order in the sequence:

$$t(k) = \frac{1}{|\mathbf{F}(k)|} \sum_{f \in \mathbf{F}(k)} t(f) \quad (20)$$

where $\mathbf{F}(k)$ is the set of features in cluster k and $t(\cdot)$ indicates the normalized temporal location. The clusters are then ordered as $\pi = [k_1, \dots, k_K]$ with respect to their temporal location, such that $0 \leq t(k_1) \leq \dots \leq t(k_K) \leq 1$. With this ordering, the transition probability is defined:

$$p(c_{n+1} | c_n) = \begin{cases} 1, & c_{n+1} = c_n \text{ or } k_{c_{n+1}} - k_{c_n} = 1, \\ 0, & \text{otherwise.} \end{cases} \quad (21)$$

Eq. (21) imposes a hard transition; new frames must either keep the same action label as the previous frame or transition to the next action label observed in the ordering π .

Comparatively, Li *et. al.* [64] define a relaxed version, taking into consideration the action length λ_c :

$$p(c_{n+1} | c_n) \propto \begin{cases} \frac{\lambda_{c_n} + \lambda_{c_{n+1}}}{\sum_{j=c_n}^{c_{n+1}} \lambda_{c_j}}, & k_{c_{n+1}} > k_{c_n}, \\ 0, & \text{otherwise.} \end{cases} \quad (22)$$

This formulation allows for the skipping of actions in the ordering π and penalizes multiple action skips with a large denominator (sum of skipped action lengths) in Eq. (22).

The second component $p(\ell | c)$, the *length model*, determines the temporal length for each action class. Common practice [21], [22], [64], [71] is to model the length of each action with a Poisson distribution:

$$p(\ell | c) = \frac{\lambda_c^\ell}{\ell!} e^{-\lambda_c}. \quad (23)$$

The lengths λ_c for actions are estimated over all video sequences by the following:

$$\hat{\lambda} = \arg \min_{\lambda} \sum_{x \in X} \left(\sum_{c \in \mathcal{A}_x} \lambda_c - T_x \right)^2, \quad \text{s.t. } \lambda_c > \lambda_{\min} \quad (24)$$

where \mathcal{A}_x is the set of occurring actions in video x with T_x frames and λ_{\min} denotes a pre-set minimum length over all actions. This ensures the minimum difference between estimated lengths by summing composing λ_c and actual length T_x over the video set and can be solved with constrained optimization by linear approximation (COBYLA) [115]. Such explicit modeling of lengths is necessary since it would avoid producing action segments that are unreasonably long.

The third component, the *visual model*, provides the probability of a feature sequence x being generated by the given action labels c . There are multiple ways to model the frame likelihood. Following Bayes' theorem, [21] proposes estimating $p(x_t | c_n)$ by considering:

$$p(x_t | c_n) \propto \frac{p(c_n | x_t)}{p(c_n)}, \quad (25)$$

where prior $p(c_n)$ can be estimated either by the fraction of frames present with label c_n [22] or as a uniform distribution for simplicity [64], while the posterior $p(c_n | x_t)$ are approximated by the output of an action classification network supervised by the action annotations.

Moreover, generative models like Gaussian Mixture Models (GMMs) can also be used to model the frame likelihood. In the GMM, the likelihood for a video frame x_t to be given an action class c_n is written as:

$$p(x_t | c_n) = \mathcal{N}(x_t; \mu_n, \Sigma_n) \quad (26)$$

where μ_n and Σ_n are the action class mean and covariance. In practice, GMMs are more preferred for cases where no action annotations are available [76], [77].

Viterbi. The MAP for the HMM described in Eq. (19) can be solved efficiently with the Viterbi algorithm [116]. Viterbi relies on dynamic programming to find the most likely sequence of states following the temporal direction. Consider the case where a uniform length model applied in Eq. (19) yields the following:

$$(\hat{N}, \hat{c}) = \arg \max_{N, c} \prod_{n=1}^{N-1} p(c_{n+1} | c_n) \cdot \prod_{t=1}^T p(x_t | c_n). \quad (27)$$

which can be further rewritten by denoting the labeling sequence of T frames π :

$$\hat{\pi} = \arg \max_{\pi} \prod_{t=1}^T p(x_t | \pi_t) \cdot p(\pi_t | \pi_{t-1}) \quad (28)$$

Given the recurrence relations, we can define the probability value $Q_{t, \hat{\pi}_t}$ of the most probable state sequence, also called the Viterbi path, as:

$$Q_{1, \pi_1} = p(x_1 | \pi_1) \cdot p(\pi_1) \quad \text{and} \quad (29)$$

$$Q_{t, \hat{\pi}_t} = \max_{\pi_t} (p(x_t | \pi_t) \cdot p(\pi_t | \pi_{t-1}) \cdot Q_{t-1, \hat{\pi}_{t-1}}). \quad (30)$$

Then Viterbi path $\hat{\pi}$ can be retrieved by traversing the saved best $\hat{\pi}_t$ from each timestamp in Eq. (30). The overall complexity of this implementation is $\mathcal{O}(T \times |N|^2)$.

Re-estimation. [64], [76] have stated that the aforementioned HMM model can be updated iteratively. As a first step, one initializes the above three HMM components with naive observations. Second, the Viterbi decoding is applied to infer the MAP label sequence. The decoded labels can again be applied to refine the feature inputs to the HMM components. These steps can be repeated until convergence.

Inference. To reduce the computational complexity of Viterbi, [117] proposed FIFA. Instead of dynamic programming, [117] define a differentiable energy function to approximate the probabilities of possible segment alignments. Their inference process reformulates the maximization of the sequence posterior by minimizing the a proposed energy function. Given the transcript $c_{1:N}$, the aim is to find the lengths $\ell_{1:N}$ correspondingly, *i.e.*,

$$\begin{aligned} \hat{\ell}_{1:N} &= \arg \max_{\ell_{1:N}} p(\ell_{1:N} | x_{1:T}, c_{1:N}) \quad (31) \\ &= \arg \min_{\ell_{1:N}} -\log p(\ell_{1:N} | x_{1:T}, c_{1:N}) \\ &= \arg \min_{\ell_{1:N}} E(\hat{\ell}_{1:N}). \end{aligned}$$

The objective energy function $E(\ell_{1:N})$ can be further decomposed as

$$\begin{aligned} E(\ell_{1:N}) &= -\log \left(\prod_{t=1}^T p(\alpha(t) | x_t) \cdot \prod_{n=1}^N p(\ell_n | c_n) \right) \\ &= \underbrace{\sum_{t=1}^T -\log p(\alpha(t) | x_t)}_{E_o} + \underbrace{\sum_{n=1}^N -\log p(\ell_n | c_n)}_{E_\ell}. \quad (32) \end{aligned}$$

where $p(\alpha(t)) = p(y_t | t; c_{1:N}, \ell_{1:N})$ is the mapping of time t to action label given the segment-wise labeling, and $c_{1:N}$ is sampled from the training set as mentioned in Section 4.3.

Two further approximations are used for the two terms in Eq. (32). First is a differentiable mask $M \in \mathbb{R}^{N \times T}$ with a parametric plateau function f [118]:

$$\begin{aligned} M[n, t] &= f(t | \lambda_n^c, \lambda_n^w, \lambda^s) \\ &= \frac{1}{(e^{\lambda^s(t - \lambda_n^c - \lambda_n^w)} + 1)(e^{\lambda^s(-t + \lambda_n^c - \lambda_n^w)} + 1)} \quad (33) \end{aligned}$$

where λ^c, λ^w are the center and lengths of a plateau computed from $\ell_{1:N}$ and λ^s is a fixed sharpness parameter. Hence, the first term E_o is approximated as:

$$E_o^* = \sum_{t=1}^T \sum_{n=1}^N M[n, t] \cdot P[n, t] \quad (34)$$

where $P[n, t] = -\log p(c_n | x_t)$ is the negative log probabilities. Secondly, for E_ℓ , c_n is replaced with the expected length value $\lambda_{c_n}^l$ based on a Laplace distribution assumption:

$$E_L^* = \frac{1}{Z} \sum_{n=1}^N |\ell_n - \lambda_{c_n}^l| \quad (35)$$

where Z is the constant normalization factor. The original energy function is finally expressed as a weighted aggregation of two approximation terms:

$$E^*(\ell_{1:N}) = E_o^*(\ell_{1:N}) + \beta E_\ell^*(\ell_{1:N}) \quad (36)$$

where β is a coefficient. FIFA can boost the inference speed up to 5 \times and at the same time maintain a comparable performance score.

6.2.2 Generalized Mallows Model

A Generalized Mallows Model models distributions over orderings or permutations. Given a set of videos belonging to the same activity, Sener *et. al.* [67] propose using a Generalized Mallows Model to model the sequential structures of actions for action segmentation. Their assumption is that a canonical sequence ordering σ is shared in these videos and they consider possible action ordering π as a permutation of σ . Such modeling offers flexibility for missing steps and deviations. A Generalized Mallows Model represents permutations as a vector of inversion counts $\mathbf{v} = [v_1, \dots, v_{K-1}]$, where K is the number of elements, *i.e.* actions, in the ordering and v_k denotes the total number of elements from $(k+1, \dots, K)$ that rank before k in the ordering π . With the distance between two orderings defined as $d(\pi, \sigma) = \sum_k \rho_k v_k$, the probability of observing \mathbf{v} is as follows:

$$P_{GMM}(\mathbf{v} | \boldsymbol{\rho}) = \frac{e^{-\sum_k \rho_k v_k}}{\psi_k(\boldsymbol{\rho})} = \prod_k \frac{e^{-\rho_k v_k}}{\psi_k(\rho_k)}, \quad (37)$$

where $\boldsymbol{\rho} = [\rho_1, \dots, \rho_{K-1}]$ is a set of dispersion parameters and $\psi_k(\rho_k)$ is the normalization function. The prior for each ρ_k is the conjugate:

$$P(\rho_k | v_{k,0}, v_0) \propto e^{-\rho_k v_{k,0} - \log(\psi_k(\rho_k)) v_0}, \quad (38)$$

A common prior ρ_0 is used for each k , such that

$$v_{k,0} = \frac{1}{e^{\rho_0}} - \frac{K - k + 1}{e^{(K-k+1)\rho_0} - 1}. \quad (39)$$

Given an action ordering π , generating frame-wise label assignment \mathbf{z} further requires an action appearance model \mathbf{a} . \mathbf{a} is the bag of action labels providing the occurrence for each action and is modeled as a multinomial parameterized by $\boldsymbol{\theta}$ and a Dirichlet prior with parameter θ_0 .

Recall that the assumption in the work of [67] is that the canonical ordering is given, thus their objective is to infer the following posterior over the entire video corpus,

$$P(\mathbf{z}, \boldsymbol{\rho} | \mathbf{F}, \theta_0, \rho_0, v_0) \propto P(\mathbf{F} | \mathbf{z}) P(\mathbf{a} | \boldsymbol{\theta}) P(\boldsymbol{\theta} | \theta_0) P(\boldsymbol{\rho} | \rho_0, v_0) \quad (40)$$

where \mathbf{F} is the frame features. The feature likelihood term $P(\mathbf{F} | \mathbf{z})$ is evaluated with GMM (Eq. (26)) and the remaining terms are approximated via MCMC sampling. Specifically, they use slice sampling for $\boldsymbol{\rho}$ and collapsed Gibbs sampling for \mathbf{z} . Similar to HMM, the above model can also be trained in two stages, where discriminative feature clustering (as described in Section 5.2.1) and sequential modeling are performed in an alternating fashion.

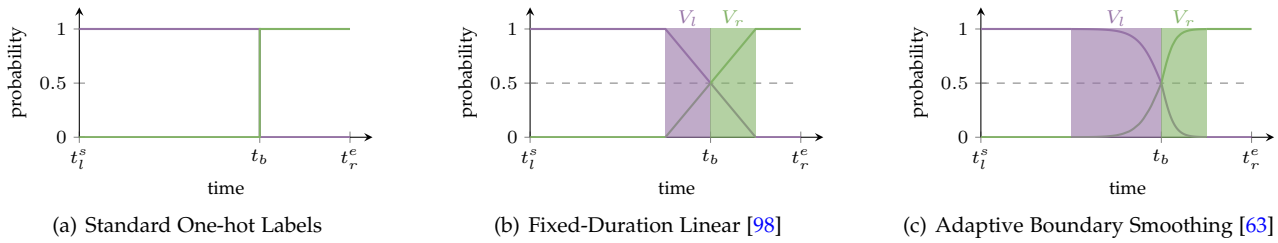


Fig. 8: Action probability assignment approaches around the action boundary as a function of time. Let t_b denote the estimated boundary between the left action in $[t_l^s, t_b)$ and the right action $[t_b, t_r^e)$. The colour-shaded segments denote the boundary vicinities V_l and V_r . (a) The standard one-hot labels adopt a step function and assign hard action labels for all the frames. (b) The fixed-duration linear approach [98] mixes the action probabilities linearly with a fixed slope around the boundary. (c) Adaptive Boundary Smoothing proposed in [63] uses a sigmoid function with a decay proportional to the action duration.

6.2.3 Dynamic Time Warping

Other than Viterbi, Dynamic Time Warping has also been adopted in the literature to implement the sequential modeling. SemiTAS [63] first sub-samples in time an ordered action sequence from the frame-wise network prediction, and then computes a cost matrix between the sequence and original network predictions to enforce the sampled sequential order of actions. The proposed continuity loss is to compute the loss along the optimal assignment path found via dynamic time warping.

6.3 Over-Segmentation

One intrinsic property of actions in procedural videos is local continuity, *i.e.*, an action should be locally constant and only transit at its actual boundary. This has prompted the researchers to improve the performance of existing segmentation algorithms by refining the results at the boundaries.

Boundary Refinement. Wang *et al.* [119] raise concerns over the boundary ambiguity and over-segmentation issues in existing works and propose a module for multi-stage segmentation algorithms [23]. Their module enables the latter stages to focus on ambiguous frames by introducing a novel Local Barrier Pooling to smooth noisy boundary predictions with confident ones. Separately, [120] proposes to complement the action segmentation branch with a boundary regression branch and utilizing the boundary detection on the segmentation outputs for label refinement during the post-processing.

Gaussian Smoothing. Smoothing with a Gaussian kernel [66], [69], [120] encourages the continuity of actions in a small local temporal window and is highly effective in boosting the overall segmentation performance, especially on the segmental metrics. While [66], [120] directly apply the smoothing on the frame-wise action probabilities, Du *et al.* [69] apply it along the temporal dimension of the sequential similarity scores between consecutive frames to mitigate the noisy frames and obtain more robust action boundaries.

Boundary Smoothing. From a different perspective, some works report that coarser and transitional action boundaries may even help boost the action segmentation performance compared to the conventional rigid ones [63], [98]. A comparison of existing boundary smoothing techniques proposed for temporal action segmentation is illustrated in Fig. 8. Correspondingly, [98] mixes the action probabilities with a fixed slope linear decay (Fig. 8(b)), while [63]

elastically expand the smoothing range to be proportional to the estimated action duration and use a sigmoid shape for mixing (Fig. 8(c)).

7 FULLY-SUPERVISED APPROACHES

Fully-supervised temporal action segmentation approach requires frame-wise action labels during training. Following the trend of other developments in action recognition, supervised action segmentation research has moved towards adapting deep learning-based solutions. Early approaches before deep-learning-based solutions to temporal action segmentation classified actions in a temporal sliding window [129], [130], [131]. Among these, Cheng *et al.* [131] reasoned on the dependencies between the actions with a Bayesian non-parametric language model. In contrast, [132], [133] modelled the actions as a change in the state of objects and treated the segmentation problem as finding change points.

Another line of methods prior to deep learning approaches predicts the most probable sequence of actions using stochastic context-free grammar to represent the temporal structure of actions [134], [135] and combining a set of hidden Markov models with a context-free grammar [47], [83]. [136] combines a visual model that maps visual features to action probabilities with a language model applied to the sequence of action segments and a length model that captures the segment durations. The final output requires dynamic programming to find the segmentation that maximizes the joint probability of the three components.

This section discusses deep models that have been used for temporal action segmentation. From a taxonomy point of view, we can identify four main categories of architectures or solutions: (1) representation learning, (2) TCN-based solutions, (3) improving existing architectures or their outputs, and (4) Transformer-based solutions.

The performance of all existing approaches is compared in Tab. 7 on the Breakfast and GTEA datasets. Overall, we observe that the majority of the approaches are based on TCNs. Although different types of features are used in the early approaches, the state of the art is mainly validated with I3D features.

7.1 Representation Learning

The earliest attempts couple deep learning-based features with temporal models. Lea *et al.* [70] employ a CNN

TABLE 7: Performance of supervised action segmentation methods validated on the Breakfast and GTEA datasets divided into three groups. The top group corresponds to approaches targeting learning better feature representations (**Feat. Rep.**). The middle group includes the methods built on Temporal Convolutional Networks (TCN). The third group aims to improve the performance of existing segmentation algorithms (**Impro.**). Lastly, the fourth group uses transformer as the backbone architecture (**TF**). We also report the features used for fair comparisons. Here, “FT” corresponds to fine-tuning, which is shown to increase the performance of segmentation. IDT corresponds to improved dense trajectories [79] and FV to Fisher vector [80] encoding along trajectories. I3D [2] features are computed on RGB and flow images.

	Method	Year	Input/Feature	GTEA					Breakfast					
				F1@{10, 25, 50}	Edit	MoF	F1@{10, 25, 50}	Edit	MoF					
Feat. Rep.	[121] Bi-LSTM	2016	RGB + flow	66.5	59.0	43.6	-	55.5	-	-	-	-	-	-
	[70] ST-CNN	2016	RGB + motion*	58.7	54.4	41.9	-	60.6	-	-	-	-	-	-
	[122] LCDC	2019	RGB	52.4	-	-	45.4	55.3	-	-	-	-	-	-
	[123] Coupled GAN	2019	RGB + flow	80.1	77.9	69.1	72.8	78.5	-	-	-	-	-	-
	[112] TempAgg	2020	I3D	-	-	-	-	-	59.2	53.9	39.5	54.5	64.5	-
TCN	[61] ED-TCN	2017	LCDC [122]	75.4	-	-	72.8	65.3	-	-	-	-	-	-
	[61] ED-TCN	2017	IDT + FV [83]	-	-	-	-	-	-	-	-	-	-	43.3
	[61] ED-TCN	2017	spatial-CNN [70]	72.2	69.3	56.0	-	64.0	-	-	-	-	-	-
	[20] TricorNet	2017	spatial-CNN [70]	76.0	71.1	59.2	-	64.8	-	-	-	-	-	-
	[99] TDRN	2018	spatial-CNN [70]	79.2	74.4	62.7	74.1	70.1	-	-	-	-	-	-
	[23] MS-TCN	2019	IDT	-	-	-	-	-	58.2	52.9	40.8	61.4	65.1	-
	[23] MS-TCN	2019	I3D (FT)	87.5	85.4	74.6	81.4	79.2	-	-	-	-	-	-
	[23] MS-TCN	2019	I3D	85.8	83.4	69.8	79.0	76.3	52.6	48.1	37.9	61.7	66.3	-
	[102] MS-TCN++	2020	I3D	87.8	86.2	74.4	82.6	78.9	64.1	58.6	45.9	65.6	67.6	-
	[124] RFGaussian	2019	I3D	88.5	86.8	74.6	84.0	78.5	62.0	56.0	43.7	63.5	64.2	-
	[125] GatedR	2020	I3D	89.1	87.5	72.8	83.5	76.7	71.1	65.7	53.6	70.6	67.7	-
	[100] C2F-TCN	2021	I3D	90.3	88.8	77.7	86.4	80.8	72.2	68.7	57.6	69.6	76.0	-
Impro.	[126] MTD + MS-TCN†	2020	I3D	90.5	88.4	76.2	85.8	80.0	74.2	68.6	56.5	73.6	71.0	-
	[127] SSTDA + MS-TCN†	2020	I3D	90.0	89.1	78.0	86.2	79.8	75.0	69.1	55.2	73.7	70.2	-
	[97] GTRM + MS-TCN**	2020	I3D	-	-	-	-	-	57.5	54.0	43.3	58.7	65.0	-
	[119] BCN + MS-TCN	2020	I3D	88.5	87.1	77.3	84.4	79.8	68.7	65.5	55.0	66.2	70.4	-
	[120] ASRF + MS-TCN	2020	I3D	89.4	87.8	79.8	83.7	77.3	74.3	68.9	56.1	72.4	67.6	-
	[128] Global2Local + MS-TCN	2021	I3D	89.9	87.3	75.8	84.6	78.5	74.9	69.0	55.2	73.3	70.7	-
	[117] FIFA + MS-TCN	2021	I3D	-	-	-	-	-	75.5	70.2	54.8	78.5	68.6	-
	[117] FIFA + ASFormer [110]	2021	I3D	90.4	88.6	78.1	86.2	78.9	76.8	71.4	58.9	75.6	73.7	-
	[117] FIFA + UVAST [111]	2022	I3D	82.9	79.4	64.7	90.5	69.8	76.9	71.5	58.0	77.1	69.7	-
	[110] ASFormer	2021	I3D	90.1	88.8	79.2	84.6	79.7	76.0	70.6	57.4	75.0	73.5	-
[111] UVAST	2022	I3D	77.1	69.7	54.2	90.5	62.2	76.7	70.0	56.6	77.2	68.2	-	

* Motion images are computed by taking the difference between frames across a 2 second window.

** The improvements are computed based on the authors’ implementation of MS-TCN.

† Test set without labels is used for training.

to capture spatio-temporal feature relations (ST-CNN) and segment videos with a semi-Markov model. Bi-LSTM [121] splits videos into snippets and passes them through a multi-stream network composed of appearance and motion streams to compute visual representation. These features are then fed into a bi-directional LSTM to predict action labels for each snippet.

Follow-up works focus on learning better representations for fine-grained actions. Instead of adding a stream for optical flow, [122] use locally consistent deformable convolutions (LCDC) to model fine-grained motion. Coupled GAN [123] uses two generative adversarial networks, one for RGB images and one for auxiliary information (depth or optical flow), to model the evolution of human actions.

TempAgg [112] is a recent multi-granular temporal aggregation framework that relates recent observations to long-range observations with attention. This network can be used for action segmentation by naively classifying snippets aggregated with long-range information. As performance is reported only over snippet scores, adding a sequence model will likely lead to further improvements.

7.2 Temporal Convolutional Networks (TCNs)

TCNs (Sec. 6.1.2) use a hierarchy of convolutions to capture long-range temporal patterns and are widely used

for temporal action segmentation. Lea *et. al.* [61] were the first to use TCNs for action segmentation. They propose an encoder-decoder architecture (ED-TCN) with 1D temporal convolutional and deconvolutional kernels that can efficiently capture long-range temporal patterns. ED-TCN’s success attracted quite some attention to the use of TCNs for temporal action segmentation, as TCNs can capture action durations, pairwise transitions, and long-term dependencies and are also faster than RNN-based solutions.

TricorNet [20] replaces the decoder in ED-TCN with a bi-directional LSTM and proposes a hybrid temporal convolutional and recurrent network. However, this network yields high computation costs due to the recurrences. TDRN [99] also builds on top of ED-TCN by replacing the temporal convolutions with deformable temporal convolutions and adding a residual stream to the encoder-decoder model. The residual stream processes videos in full temporal resolution, while the other stream captures the temporal context at different scales.

Although the aforementioned approaches based on TCNs work on the entire video – referred to as *full resolution* – these methods, in practice, temporally downsample the videos to a few frames per second. Such pre-processing may cause a loss of fine-grained details. In contrast, Farha and Gall [23] propose a multi-stage hierarchical temporal

convolutional network, namely MS-TCN, that works on exact full-resolution video. In MS-TCN, each stage consists of multiple temporal convolutional layers with 1D dilated convolutions and outputs an initial prediction, which is iteratively refined by the following stages. This work improves the segmentation performance compared to previous works [61], [99] by a large margin and significantly reduces the over-segmentation errors.

To improve on MS-TCN, MS-TCN++ [102] shares the parameters in the refinement stages and introduces a dual dilated layer to capture both local and global features. RPGaussian [124] introduces a bilinear pooling module that can be integrated into TCNs to serve as a computationally efficient feature fusion operation, *e.g.*, by replacing the last 1×1 convolution layer in the first stage of MS-TCN [23]. GatedR [125] uses a gated forward refinement network to adaptively correct errors from the previous stages. It also includes a multi-stage sequence-level refinement loss to correct the errors in the previous predictions.

Recently, analyzing the fragmentation issues in TCNs, Singhania *et al.* [100] proposed an encoder-decoder model with a coarse-to-fine ensemble of decoding layers, C2F-TCN. The ensemble of these decoder outputs is less fragmented and more accurate. This work also presents a multi-resolution feature-level augmentation strategy and an action loss, which penalizes misclassifications at the video level, improving the segmentation performance.

7.3 Improving Existing Architectures or Outputs

Several works focus on improving existing temporal action segmentation algorithms by integrating new modules into existing backbones or post-processing the outputs. Chen *et al.* [127] argue that spatio-temporal variations of human actions – referred to as *different domains* – cause low performance in supervised action segmentation, as training a model in one domain and testing it in another will fail due to the variation across videos. They propose using two self-supervised auxiliary tasks to decrease differences between the feature spaces of the source and target domains. One task predicts which domain a single frame’s feature vector comes from, while the other predicts domain labels for a shuffled *sequence* of source and target segments. Integrating their self-supervised model, SSTDA, to MS-TCN significantly improves the action segmentation performance without using additional labeled data. Such superior performance could also benefit from access to the test data as the unlabeled inputs.

GTRM [97] refines segmentation outputs from existing action segmentation algorithms with a graph convolutional network (GCNs). The extent of refinement depends on the initial segmentation’s quality and degree of fragmentation. Temporal receptive fields in segmentation models are crucial, whereby large fields facilitate long-term relations while small receptive fields help capture the local changes. Instead of using hand-designed receptive fields, Global2Local [128] introduces a search scheme of effective receptive field combinations that can be plugged into any existing segmentation model.

Another emerging idea for improvement is to correct segmentation results at action boundaries. Wang *et al.* [119]

raise concerns over the boundary ambiguity and over-segmentation issues in existing works and specifically propose a module that can be used with multi-stage segmentation algorithms [23]. Their module, BCN, enables the later stages to focus on ambiguous frames. A newly introduced pooling operator smooths noisy boundary predictions with confident ones. Similarly, ASRF [120] also performs boundary refinement, though it is model-agnostic and can be applied to any action segmentation output.

Finally, FIFA [117], a general inference method, can be applied at test time on top of existing segmentation approaches for fast inference. FIFA improves the speed by more than five times while maintaining the performance of backbone architectures.

7.4 Transformers

Recently, transformers have been utilized for temporal action segmentation. ASFormer [110] is a transformer-based segmentation model composed of an encoder and several decoders to perform iterative refinement. A self-attention block with instance normalization is used per dilated temporal convolutional layer of MS-TCN. The first stage is the encoder, which receives the video sequences and outputs initial predictions, and the decoders get the predictions from the previous layers as the input. ASFormer performs on par with MS-TCN on GTEA while outperforming it on Breakfast.

Another recent work, UVAST [111], uses a similar encoder to ASFormer and a different decoder. Unlike ASFormer and MS-TCN, which perform frame-level predictions, UVAST’s decoder predicts the action segments in an auto-regressive manner. UVAST outperforms the previous methods on Edit Score and F1-score, indicating less over-segmentation.

8 WEAKLY-SUPERVISED APPROACHES

Weakly-supervised approaches target avoiding dense frame-level supervision. We divide such methods into five categories. One group receives supervision as an ordered list of actions called *transcripts*. The second one uses an unordered list of actions called *action sets*. The third group uses a single-frame label for each action. The fourth is an even weaker supervision form where only the complex activity labels are used as input. The fifth and last category is the group of segmentation methods that use complementary *textual data* such as narrations to provide temporal constraints for segmentation. We compare the performance of all existing approaches in Tab. 8 for the Breakfast and 50Salads datasets.

8.1 Transcripts: Ordered List of Actions

Kuehne *et al.* [137] were the first to use the term *transcripts* to refer to an ordered list of the actions occurring in a video. Even earlier work already features transcripts [138], though they target aligning frames with the transcripts and assume that transcripts of the test sequences are also provided. Transcript-based supervision, however, provides only the actions within a video and the order in which they occur.

This type of supervision significantly reduces the cost of annotating videos as it does not require any frame-wise labels and could speed up the annotation by $8\times$ with the Breakfast dataset. We group these methods into two categories of iterative two-stage and single-state solutions.

8.1.1 Iterative Two-Stage Solutions

The two-stage solutions start with an initial estimate of frame-wise labels and then iteratively improve them with a segmentation model. These approaches follow an iterative refinement of previous predictions to segment videos. HTK [137] extends a supervised approach from a supervised approach [83] to a weakly-supervised setting. In this framework, the actions are modeled by a set of HMM, while GMM models the observations. The algorithm uniformly initializes the video segments based on the transcripts and iteratively refines them. Richard *et. al.* [96] build on this idea and replace GMMs with recurrent neural networks. They also further divide the actions into snippets to capture their finer-detailed characteristics.

The Temporal Convolutional Network based approach ISBA [98] extends the TCN from [61] by adding lateral connections between the encoder and decoder layers. They use a soft labeling mechanism at the segment boundaries and iteratively refine the segmentation. TASL [139] proposes to model the actions subspaces with an ensemble of auto-encoders together with a similar two-stage strategy of iterating between aligning videos with respect to transcripts and learning subspace learning with the alignment. Specifically, a constrained Viterbi decoding algorithm [21], [71] is utilized to solve the alignment problem efficiently.

8.1.2 Single-Stage Solutions

The two-step approaches are sensitive to initialization and may not converge as the models are learned incrementally. Single-stage approaches allow for the direct learning of segmentation. ECTC [140] is an extended version of connectionist temporal classification [141] for aligning the transcripts with video frames with consistency constraints. It enforces frame-wise similarities to be consistent with the action alignments. This reduces the space of possible paths and avoids degenerate segmentation, which might occur due to the large number of frames in long videos.

NN-Viterbi [21] uses Viterbi decoding as part of the loss function to train a segmentation network. The Viterbi algorithm generates pseudo-ground truths over the output probabilities of the network, which are then used to compute the loss. This method provides significant improvements over the previous methods. However, it is costly to train due to Viterbi decoding. Chang *et. al.* [142] propose D^3TW , a framework with a differentiable alignment loss to model positive and negative transcripts discriminatively. A similar discriminative training is proposed by Li *et. al.* [143], who build their framework, CDFL, on NN-Viterbi with ordering constraints. Unlike the randomly selected negative transcripts of D^3TW , CDFL generates valid and invalid segmentation candidates using a segmentation graph, where invalid candidates violate the transcripts. It recursively estimates each candidate's segmentation energy and formulates a new loss based on the energy differences between valid and invalid candidates. CDFL shows improved performance

over previous works by a significant margin; however, its training is more expensive.

Souri *et. al.* [144] point out the long training times of the state-of-the-art and employ a sequence-to-sequence network that performs comparably to earlier works but is much faster during training and inference. Their framework, Mu-Con, is composed of two branches, where one predicts transcripts and action durations, while the other outputs frame-wise predictions. The predictions from the two branches are used to compute a mutual consistency loss to enforce similar predictions. A recent work, DP-DTW [145], learns class-specific discriminative action prototypes for weakly-supervised segmentation and proposes that videos could be represented by concatenating prototypes according to transcripts. The model aims at increasing the inter-class difference among prototypes via discriminative losses.

8.2 Action Set

In this setting, the methods assume that a set of action labels is provided during training without knowing the temporal location, the order, or how often they occur. This type of labeling can arise in the form of meta-tags *e.g.*, from video-sharing platforms.

Richard *et. al.* [22] are the first to propose a weak segmentation model using action sets. Similar to [136], their framework has an action, length, and sequence component and uses Viterbi to find the most likely segmentation. They generate multiple transcripts using context-free grammars to restrict the search space and convert the problem into a weakly-supervised segmentation setting with multiple transcripts. However, this work cannot generate all possible sequences of a set of action labels, which might degrade segmentation quality.

SCT [146] learns a segmentation network that directly uses provided annotations for learning. They start by splitting videos into regions and estimate action probabilities and temporal lengths for them in one branch. They use a second branch to produce frame-wise predictions. They measure the consistency of the frame-wise predictions with respect to region predictions, which significantly improves the model's accuracy. They also define several losses and regularizers to encourage temporally consistent predictions between neighboring regions or regularize region lengths.

SCV [71] uses a set-constrained Viterbi algorithm to generate accurate pseudo ground truths and an n -pair loss to minimize the distance between pairs of training videos sharing action classes in their action sets. It uses a greedy post-processing step to ensure that all the set actions are included in the frame-wise pseudo-ground truth by changing the frame labels with low scores to action labels present in the action set but not in the initial segmentation. ACV [147] improves this work by removing the need for post-processing via a differentiable approximation which allows end-to-end training. It constructs an anchor-constrained graph and estimates anchor segments to constrain the set of valid candidate sequences.

Recently, Lu *et. al.* [148] observed that it is common for action pairs to have a fixed temporal order in several procedural video datasets, which could help boost the segmentation performance. Accordingly, they incorporated such

TABLE 8: Performance of weakly supervised action segmentation methods validated on the Breakfast and 50Salads datasets. The first and second groups correspond to approaches using transcripts (**Tr.**). The first group lists methods following an iterative two-stage solution (**T**), and the methods in the second group propose a single-stage solution (**S**). The third group uses action set as the weak supervision (**Set**), and the fourth group expects a single timestamp for each action as supervision (**TS**), while the last group only uses complex activity labels (**CA**). IDT corresponds to improved dense trajectories [79] and FV to Fisher vector [80] encoding along trajectories. The I3D [2] features are computed on RGB and optical flow.

	Method	Year	Feature	Breakfast			50Salads
				MoF	IoU	IoD	MoF
Tr. + T	[137] HTK	2017	IDT + FV	25.9	-	-	24.7
	[96] HMM/RNN	2017	IDT + FV	33.3	-	-	45.5
	[98] ISBA	2018	IDT + FV	38.4	24.2	40.6	-
	[139] TASL	2021	IDT + FV	49.9	36.6	34.3	-
Tr. + S	[140] ECTC	2016	IDT + FV	27.7	-	-	-
	[21] NN-Viterbi	2018	IDT + FV	42.9	32.2	29.1	49.4
	[142] D ³ TW	2019	IDT + FV	45.7	-	-	-
	[143] CDFL	2019	IDT + FV	50.2	33.7	45.4	54.7
	[144] MuCon	2019	IDT + FV	48.5	-	-	-
	[145] DP-DTW	2021	IDT + FV	50.8	35.6	45.1	-
Set	[22] ActionSet	2018	IDT + FV	23.3	-	-	-
	[146] SCT	2020	IDT + FV	26.6	-	-	-
	[146] SCT	2020	I3D	30.4	-	-	-
	[71] SCV	2020	IDT + FV	30.2	-	-	-
	[147] ACV	2021	IDT + FV	33.4	-	-	-
TS	[149] Timestamps	2021	I3D	64.1	-	-	75.6
	[65] EM-TSS	2022	I3D	63.7	-	-	75.9
CA	[66] CAD	2022	IDT+FV	49.5	-	-	-
	[66] CAD	2022	I3D	53.1	-	-	-

constraints into learning with a pairwise order consistency loss. The loss penalizes the ordering disagreement between pre-extracted templates and segmentation model outputs.

8.3 Single-Frame Supervision

Instead of annotating every frame with an action label, another type of supervision is obtaining labels from single timestamps for each action, significantly reducing the annotation effort. The single timestamp could be any arbitrary frame for each segment.

Li *et al.* [149] propose a method for generating frame-wise labels by detecting the action changes. They also introduce a confidence loss that enforces the class probabilities to decrease monotonically as the distance to the timestamp increases. Their approach can be applied to any action segmentation model, *e.g.*, MS-TCN, for training using timestamps annotations only. Compared to using transcripts or action set-based weak supervision, this type of supervision improves the segmentation performance significantly. It performs comparably to the fully-supervised approaches, making it an exciting direction to explore weak supervision.

Recently, Rahaman *et al.* [65] proposed integrating Expectation-Maximization (EM) for timestamp supervision with the intuition that the unobserved frame labels can be considered missing and inferred from the labeled timestamps. The E-step is defined to train the network for the label estimation, while the M-step maximizes the timestamp segment likelihood and finds the boundary accordingly. They further demonstrate the generalizability of the proposed EM approach to handle the missing actions in-between annotated timestamps. Their model, EM-TSS, also shows that only labeling the initial frame for each segment

degrades the performance compared to a random or middle frame initialization, indicating the ambiguities of labels at the boundaries.

The previously discussed approaches use a segmentation model to help infer the action boundaries that are in between timestamps, while GCN [150] proposed to adopt instead the Graph Neural Network (GNN) to achieve the same purpose in an alternative manner. Specifically, the frame features are treated as node and the edges between consecutive frames are weighted by their feature affinity computed as the cosine similarity. The GNN is trained to propagate labels from only a few labeled nodes to the remaining unlabeled nodes.

8.4 Narrations & Subtitles

Video is often accompanied by freely available text data in the form of scripts, subtitles, or narrations. It is frequently used for video and text alignment [57], [151] and step localization [25], [35]. Several works make use of text to weakly supervise action segmentation. The main disadvantage of models employing textual data is the assumption that *all* the videos are accompanied by temporally aligned text. However, text data might not always be aligned or may even be completely missing.

Sener *et al.* [152] use visual and language cues in a joint generative model to perform video segmentation. They first generate object proposal segments from a collection of videos of the same activity and compute visual vocabularies. Using those together with textual vocabularies computed over narrative text, they represent each frame with a binary histogram over visual and textual words. To identify the actions shared among the videos, they utilize the generative beta process mixture model from [34], but on binary observations. They evaluate the proposed method on a newly collected dataset including 17 activities and 5 test videos annotated per activity.

On a separate track, Fried *et al.* [53] propose an approach that uses canonical step ordering and transcribed narrations in videos as supervision for segmentation. Canonical step ordering refers to the sequence in which the steps of activities are typically performed. Using a semi-Markov model, they model the segment duration, location, order, and features. Although they do not use the narrations during testing, they use the canonical ordering during inference, as these constraints affect their model parameters. This work systematically evaluates how much models can improve when increasing the amount of supervision, *e.g.*, from solely using canonical ordering to using transcripts from narrations or full supervision. They only report results for the CrossTask dataset [35], as it includes narrations and canonical orderings for activities, which allow for their systematic evaluation.

8.5 Activity Supervision

An even weaker supervision signal proposed for the action segmentation task is to use only the complex activity labels [66]. This type of supervision does not provide any action-level information. Under this setting, Ding and Yao [66] propose a Constituent Action Discovery (CAD) framework that learns frame representations in terms of

TABLE 9: Performance of unsupervised action segmentation methods evaluated on the Breakfast Actions dataset. The methods in the top group do not use self-supervision and are composed of two stages (**Two Stg.**). The middle group includes methods using self-supervision (**SS**). The last group list methods operating in a single stage (**Single Stg.**). IDT corresponds to improved dense trajectories [79] and FV to Fisher vector [80] encoding along trajectories. **F1(A)** and **MoF(A)** correspond to Hungarian matching computed on activity level, and **MoF(V)** is computed on the video level. The reported numbers are for the setting where the activity label and the number of actions are given as input. We also present how **Temporal Model** is defined and their flexibility for allowing **Deviations**, **Missing** steps and **Repetitions** in orderings.

	Method	Year	Input/Feature	F1(A)	MoF(A)	MoF(V)	Temporal Model	Deviations	Missing	Repetitions
Two Stg.	[67] Mallows	2018	IDT + FV	-	34.6	-	Mallows model [153]	✓	✓	-
	[154] Prism	2019	IDT + FV	-	33.5	-	hierarchical Bayesian model	-	-	✓
	[76] CTE	2019	IDT + FV	26.4	41.8	-	temporal cluster order	-	✓	-
	[77] JVT	2021	IDT + FV	29.9	48.1	52.2	temporal cluster order	-	✓	-
	[66] CAD*	2021	IDT + FV	-	49.5	-	temporal cluster order	-	✓	-
	[66] CAD*	2021	I3D	-	53.1	-	temporal cluster order	-	✓	-
SS	[64] ASAL	2021	IDT + FV	37.9	52.5	-	HMM	-	✓	-
	[155] CAP	2021	SpeedNet [156]	39.2	51.1	-	temporal cluster order	-	✓	✓
Single Stg.	[75] LSTM+AL	2019	CNN [157]	-	-	42.9	-	-	-	-
	[158] UDE	2021	I3D	31.9	47.4	74.6	temporal cluster order	-	✓	-
	[159] TOT	2021	IDT + FV	31.0	47.5	-	temporal optimal transport	-	✓	-
	[68] TW-FINCH	2021	IDT + FV	-	-	62.7	-	-	-	-
	[69] ABD	2022	IDT + FV	-	-	64.0	-	-	-	-

* CAD is included here as it essentially uses same amount of supervision information as the unsupervised approaches.

their similarity with respect to the latent action prototypes. They assume that aggregated action prototype affinities over the whole video sequence can be used to infer the complex activity label. Despite being considered weakly supervised, this method exploits the same amount of supervision information as most unsupervised works. Therefore, this approach is evaluated via Hungarian matching as described in Section 4.4.

9 UNSUPERVISED APPROACHES

Unsupervised action segmentation approaches do not require any action labels, temporal boundaries, or textual data for supervision. However, they would implicitly require the activity information because of the application scope of their proposed learning strategies [67], [76], [152].

Tab. 9 categories existing unsupervised works and compares their performances on the Breakfast dataset. The first group of works [67], [76], [77] follows two iterative stages by alternating between estimating the frame clusters and updating the frame representations. There have been continuous efforts to improve the state-of-the-art by using self-supervised learning-based representations [64], [155]. The last group disregards the sequence dynamics and performs segmentation only based on boundary changes, *e.g.* LSTM+AL [75], TW-FINCH [68] and ABD [69]. Surprisingly these methods outperform previous works on unsupervised temporal segmentation. This is likely due to the limitations in the existing datasets, which are either too small to observe the influence of modeling the sequence structure [45] or have actions that mostly follow a strict ordering [47].

9.1 Two-Stage Learning

Sener and Yao [67] are the first to propose an unsupervised segmentation approach that works solely with visual data without any supervision. They propose an iterative discriminative-generative approach to segment videos. Their method alternates between discriminatively learning the appearance of actions and generatively modelling their temporal structure using a Generalized Mallows Model [153], which models the distribution over action

permutations. Following this work, there has been recent interest in the unsupervised segmentation of videos. [67] assumes a collection of videos, all of the same activity, and with the total number of actions. Follow-up works also follow this setting.

Although the Mallows framework allows for deviations from ordering, such as missing steps, it cannot model repeated actions since the ordering of actions is treated as a sequence of permutable steps. Follow-up works on unsupervised learning are therefore evaluated according to their flexibility in deviations, missing steps and repetitions in orderings. For example, Prism [154] is a generative hierarchical Bayesian model that allows for repeated actions. However, this model assumes that all the videos follow the same underlying ordering.

The majority of the recent works, CTE [76], JVT [77], ASAL [64], UDE [158] and TOT [159], achieve higher performance compared to the Mallows [67] framework (see Tab. 9). In practice, CTE [76] first learns continuous temporal embeddings of frame-wise features. These features are then clustered, and the video ordering is decoded according to the ordered clusters of embedded features using the Viterbi algorithm. CTE has a variant that groups videos into activity clusters in a pre-processing stage instead of getting the activity labels as input. JVT [77] is a joint visual-temporal learning model using the temporal embedding from CTE and an encoder-decoder network predicting the features of subsequent frames. These two embedding networks are, in turn, trained in a joint framework to learn useful representations of visual and temporal attributes. The embedding space is then used for clustering to form the action segments, similar to CTE [76].

The above methods assume a fixed sequential ordering determined by computing the mean timestamp of each cluster. Using a fixed order for all videos allows missing steps but cannot accommodate sequence deviations or action repetitions. CAP [155] specifically targets these shortcomings and proposes a method for computing the video order by representing the multi-occurrence of actions using co-occurrence relations. Recently, Bansal *et. al.* [160] proposed to infer the temporal orderings of the discovered actions per

TABLE 10: Performance of semi-supervised action segmentation methods evaluated on GTEA, Breakfast Actions and 50Salads with varying ratios of labeled data (D%). Abbreviated names are feature learning (FL) that learns a new set of inputs in a self-supervised manner, test data (TD) is used for feature learning, and feature ensembling (FE) technique to boost the performance. Complex acvity indicates the video-level labels used for training (CA), which is only applicable to the Breakfast dataset.

D%	Method	Year	FL	TD	FE	Backbone	Breakfast					50Salads					GTEA					
							CA	F1@{10, 25, 50}			Edit	Acc	F1@{10, 25, 50}			Edit	Acc	F1@{10, 25, 50}			Edit	Acc
5%	[63] SemiTAS	2022	-	-	-	MS-TCN [23]	-	44.5	35.3	26.54	45.9	38.1	37.4	32.3	25.5	32.9	52.3	59.8	53.6	39.0	55.7	55.8
	[63] SemiTAS	2022	-	-	-	MS-TCN [23]	✓	56.6	49.3	35.8	59.4	56.6	-	-	-	-	-	-	-	-	-	
	[62] ICC	2022	✓	✓	✓	ED-TCN [61]	-	-	-	-	-	-	39.3	34.4	21.6	32.7	46.4	-	-	-	-	
	[62] ICC	2022	-	-	✓	C2F-TCN [62]	-	-	-	-	-	-	42.6	37.5	25.3	35.2	53.4	-	-	-	-	
	[62] ICC	2022	✓	✓	✓	C2F-TCN [62]	✓	60.2	53.5	35.6	56.6	65.3	52.9	49.0	36.6	45.6	61.3	77.9	71.6	54.6	71.4	68.2
10%	[63] SemiTAS	2022	-	-	-	MS-TCN [23]	-	56.9	51.3	39.0	57.7	49.5	47.3	42.7	31.8	43.6	58.0	71.5	66.0	52.9	67.2	62.6
	[62] ICC	2022	✓	✓	✓	C2F-TCN [62]	✓	64.6	59.0	42.2	61.9	68.8	67.3	64.9	49.2	56.9	68.6	83.7	81.9	66.6	76.4	73.3

video based on the intuition that they could be multiple ways of performing a certain task. However, in [160], the ordering is still determined based on the mean cluster timestamps identical to [76].

9.2 Self-Supervised Learning

Self-supervised learning is shown to perform superior to the current state-of-the-art features on tasks such as image classification and action recognition [161]. Wang *et al.* [155] propose using various self-supervised learning methods to extract frame-level feature representation in unsupervised learning. Similar to exiting unsupervised works [76], [77], they first cluster these features. Their method, CAP, decodes the frames into actions considering the temporal order of actions and their co-occurrence relations. This allows for better modeling of the underlying structure of activities and, therefore, the repetitions. They also compare various self-supervision architectures, showing that such feature-learning methods can effectively improve performance.

ASAL [64] presents an effective method for the self-supervised learning of feature embeddings by the temporal shuffling of the predicted action segments and classifying the action sequences as valid and invalid. The segmentation method alternates between training an HMM using pseudo ground truths actions and predicting these latent actions.

9.3 Single-Stage Learning

Previous works are composed of an embedding stage where a joint space is learned based on visual and/or temporal information and a clustering stage applied to the embedded features. Another line of work performs segmentation in a single stage. Aakur *et al.* [75] propose a self-supervision-based approach to detect action boundaries through only a single pass on the training data. Their model LSTM+AL recurrently predicts features of the next frame and computes the difference to the observed features to determine action boundaries.

Swetha *et al.* [158] propose an approach, UDE, for jointly learning embedding and clustering. Their latent embedding space combines visual and positional encoding, and they use contrastive learning for clustering. Kumar *et al.* [159] also combines representation learning and clustering into a single joint framework, TOT. They use a combination of temporal optimal transport to preserve the temporal order of actions and temporal coherence loss for embedding nearby frames close to each other.

A recent work, TW-FINCH [68], encodes the spatio-temporal similarities between frames and uses a temporally

weighted hierarchical clustering approach to group semantically consistent frames in the videos. This approach does not require a training stage as it can be used to find action boundaries directly based on the pre-computed features. A similar work that does not require training is ABD [69], which detects abrupt change points as the action boundaries based on the similarity calculated directly on the raw input feature vectors.

10 SEMI-SUPERVISED APPROACHES

Compared to the methods using weak supervision that require annotation for *every* video instance in the training set, semi-supervised training only requires dense labeling for a small *subset* of videos. Ding and Yao [63] show that a small subset of dense annotations provides more information than single-frame supervision on the entire dataset. They argue that such supervision provides not only frame-level action class information but also valuable action-level prior information to guide the learning of the unlabeled videos. Their model, SemiTAS [63], introduces two novel losses for semi-supervised temporal action segmentation, *i.e.*, action affinity loss and action continuity loss. Specifically, the affinity loss imposes the action composition and distribution prior on the video level by minimizing the KLD between the closest label-unlabeled video pair.

Similarly, ICC [62] proposes a semi-supervised method for temporal action segmentation. ICC learns frame-wise representations using TCNs by clustering input features. The unlabeled videos are supervised by the pseudo-labels generated by the network outputs. With 40% labeled data, ICC performs comparably to the fully-supervised counterparts. We provide detailed performance comparisons in Tab. 10.

11 CONCLUSIONS AND OUTLOOK

This survey gave an overview of the methods used in temporal action segmentation, followed by a comprehensive review of the literature at the time of this writing. The extensive body of literature shows the growing interest in the topic. Despite the rapid development in the field, there are still several open topics that we encourage the community to investigate.

Input Features. The mainstream works on action segmentation take visual feature vectors, either hand-crafted (IDT) [79] or extracted from an off-the-shelf CNN backbone (I3D) [2], as input for each frame. Using pre-computed features as inputs serves as a conventional practice for

several other tasks as well, including temporal action localization [10], [11], action anticipation [15], [19], as it greatly reduces the computational demands and advocates a dedicated comparison of architectures, removing the impact of enhanced feature representations.

However, as pointed out by [91], [92], pre-computed features might create a bias towards the static cues, e.g. scene components, in frames. To the best of our knowledge, no empirical study has thoroughly compared pre-computed features to training from raw images in an end-to-end way, as it is highly challenging in terms of training efficiency and GPU memory requirements.

Segment-Level Modeling. As we have discussed in Section 6.2, almost all of the current methods for the sequential modeling of actions are performed in an iterative way, which is separated from feature learning. Besides, there has also been a heavy reliance on exploiting temporal modeling techniques to post-process and refine the per-frame outputs. One promising yet under-explored direction is to explore how to incorporate the sequence-related losses, e.g., edit score penalizing segment-wise errors, as a part of the learning. Imposing segment-level loss naturally aligns with the first interpretation of the action segmentation task, as we described with Eq. (1). We also advocate more efforts addressing the task from the action segment level as the majority of existing approaches work with a frame-wise prediction perspective as defined in Eq. (2).

Forms of Supervision. Procedural video sequences contain massive temporal redundancies in the supervisory signals. Temporal redundancy is due to the significant similarity between successive video frames of the same action. Such redundancy has been validated by the comparable performance of using single-frame supervision vs. fully-supervised setting [65], [149]. However, even single-frame supervision requires a careful annotator to skim through every video to ensure no actions are missed. Although briefly investigated in [65], how to deal with missing actions in annotations would be a possible direction for temporal action segmentation.

Another aspect to consider in terms of supervision is the inherent ambiguity of the action boundaries in procedural videos during annotation, as actions occurring in time are oftentimes not as clean cut as an object in space. As reported by [63], these ambiguities in action boundaries could greatly affect the model performance. Hence, it is worth exploring how to define/label action boundaries.

Downstream tasks Temporal segmentation outputs can also be used in downstream tasks. For example, Soran *et al.* [162] segments video streams to issue notifications about missing actions, e.g., ‘turn off the oven’. Rivoir *et al.* [163] employ segmentation as a preliminary task for predicting the remaining time of long surgery videos. Similarly, in action anticipation, several approaches utilize segmentation methods to represent past observations with action labels [164], [165], [166]. This is because such labels contain high-level semantic information, which is preferable to visual features for anticipation tasks [112]. Similarly, having obtained high-level semantic results from an action segmentation method, an intelligent system can summarize the contents of a video, i.e., video summarization [167].

Furthermore, shifting the temporal action segmentation

towards an online setting could make such techniques more applicable for applications in the real world. The very first attempts towards this goal were made in [69], [168]. However, both methods rely on pre-computed frame-wise features. A future direction could be online segmentation of videos with end-to-end models.

In conclusion, temporal action segmentation is a promising and fast-developing research field with many potential real-world applications. In this survey, we provide a detailed taxonomy of the task, systematically review the core techniques, and curate a comprehensive list of existing works categorized by levels of supervision. We further point out the opportunities as well as the challenges ahead. We hope that this survey will provide an exposition of this topic, datasets, fair evaluations, and promote the growth of the community.

REFERENCES

- [1] S. Minaee, Y. Y. Boykov, F. Porikli, A. J. Plaza, N. Kehtarnavaz, and D. Terzopoulos, “Image segmentation using deep learning: A survey,” *IEEE Transactions on Pattern Analysis and Machine Intelligence*, 2022.
- [2] J. Carreira and A. Zisserman, “Quo vadis, action recognition? a new model and the kinetics dataset,” in *IEEE Int. Conf. on Computer Vision and Pattern Recognition*, 2017, pp. 6299–6308.
- [3] C. Feichtenhofer, H. Fan, J. Malik, and K. He, “Slowfast networks for video recognition,” in *Int. Conf. on Computer Vision*, 2019, pp. 6202–6211.
- [4] J. Lin, C. Gan, and S. Han, “Tsm: Temporal shift module for efficient video understanding,” in *Int. Conf. on Computer Vision*, 2019, pp. 7083–7093.
- [5] M. Patrick, D. Campbell, Y. Asano, I. Misra, F. Metze, C. Feichtenhofer, A. Vedaldi, and J. F. Henriques, “Keeping your eye on the ball: Trajectory attention in video transformers,” *Advances in Neural Information Processing Systems*, vol. 34, pp. 12 493–12 506, 2021.
- [6] J. Carreira, E. Noland, C. Hillier, and A. Zisserman, “A short note on the kinetics-700 human action dataset,” *arXiv preprint arXiv:1907.06987*, 2019.
- [7] M. Monfort, A. Andonian, B. Zhou, K. Ramakrishnan, S. A. Bargal, T. Yan, L. Brown, Q. Fan, D. Gutfreund, C. Vondrick *et al.*, “Moments in time dataset: one million videos for event understanding,” *IEEE Transactions on Pattern Analysis and Machine Intelligence*, vol. 42, no. 2, pp. 502–508, 2019.
- [8] E. Elhamifar and D. Huynh, “Self-supervised multi-task procedure learning from instructional videos,” in *European Conf. on Computer Vision*, 2020.
- [9] Z. Naing and E. Elhamifar, “Procedure completion by learning from partial summaries,” in *British Machine Vision Conference*, 2020.
- [10] Z. Shou, D. Wang, and S.-F. Chang, “Temporal action localization in untrimmed videos via multi-stage cnns,” in *IEEE Int. Conf. on Computer Vision and Pattern Recognition*, 2016, pp. 1049–1058.
- [11] Y. Xiong, Y. Zhao, L. Wang, D. Lin, and X. Tang, “A pursuit of temporal accuracy in general activity detection,” *arXiv preprint arXiv:1703.02716*, 2017.
- [12] P. V. K. Borges, N. Conci, and A. Cavallaro, “Video-based human behavior understanding: A survey,” *IEEE Transactions on Circuits and Systems for Video Technology*, vol. 23, no. 11, pp. 1993–2008, 2013.
- [13] S. Vishwakarma and A. Agrawal, “A survey on activity recognition and behavior understanding in video surveillance,” *The Visual Computer*, vol. 29, no. 10, pp. 983–1009, 2013.
- [14] H.-B. Zhang, Y.-X. Zhang, B. Zhong, Q. Lei, L. Yang, J.-X. Du, and D.-S. Chen, “A comprehensive survey of vision-based human action recognition methods,” *Sensors*, vol. 19, no. 5, p. 1005, 2019.
- [15] Y. Kong and Y. Fu, “Human action recognition and prediction: A survey,” *International Journal on Computer Vision*, vol. 130, no. 5, pp. 1366–1401, 2022.
- [16] H. Xia and Y. Zhan, “A survey on temporal action localization,” *IEEE Access*, vol. 8, pp. 70 477–70 487, 2020.

- [17] A. Baraka and M. H. Mohd Noor, "Weakly-supervised temporal action localization: a survey," *Neural Computing and Applications*, pp. 1–21, 2022.
- [18] N. P. Trong, H. Nguyen, K. Kazunori, and B. Le Hoai, "A comprehensive survey on human activity prediction," in *International Conference on Computational Science and Its Applications*. Springer, 2017, pp. 411–425.
- [19] A. Rasouli, "Deep learning for vision-based prediction: A survey," *arXiv preprint arXiv:2007.00095*, 2020.
- [20] L. Ding and C. Xu, "Tricornet: A hybrid temporal convolutional and recurrent network for video action segmentation," *arXiv preprint arXiv:1705.07818*, 2017.
- [21] A. Richard, H. Kuehne, A. Iqbal, and J. Gall, "Neuralnetworkviterbi: A framework for weakly supervised video learning," in *IEEE Int. Conf. on Computer Vision and Pattern Recognition*, 2018, pp. 7386–7395.
- [22] A. Richard, H. Kuehne, and J. Gall, "Action sets: Weakly supervised action segmentation without ordering constraints," in *IEEE Int. Conf. on Computer Vision and Pattern Recognition*, 2018, pp. 5987–5996.
- [23] Y. A. Farha and J. Gall, "Ms-tcn: Multi-stage temporal convolutional network for action segmentation," in *IEEE Int. Conf. on Computer Vision and Pattern Recognition*, 2019, pp. 3575–3584.
- [24] B. Krüger, A. Vögele, T. Willig, A. Yao, R. Klein, and A. Weber, "Efficient unsupervised temporal segmentation of motion data," *IEEE Transactions on Multimedia*, vol. 19, no. 4, pp. 797–812, 2016.
- [25] J.-B. Alayrac, P. Bojanowski, N. Agrawal, J. Sivic, I. Laptev, and S. Lacoste-Julien, "Unsupervised learning from narrated instruction videos," in *IEEE Int. Conf. on Computer Vision and Pattern Recognition*, 2016.
- [26] T. Lin, X. Zhao, H. Su, C. Wang, and M. Yang, "Bsn: Boundary sensitive network for temporal action proposal generation," in *European Conf. on Computer Vision*, 2018, pp. 3–19.
- [27] T. Lin, X. Liu, X. Li, E. Ding, and S. Wen, "Bmn: Boundary-matching network for temporal action proposal generation," in *Int. Conf. on Computer Vision*, 2019, pp. 3889–3898.
- [28] Y.-G. Jiang, J. Liu, A. Roshan Zamir, G. Toderici, I. Laptev, M. Shah, and R. Sukthankar, "THUMOS challenge: Action recognition with a large number of classes," <http://crcv.ucf.edu/THUMOS14/>, 2014.
- [29] F. Caba Heilbron, V. Escorcia, B. Ghanem, and J. Carlos Niebles, "Activitynet: A large-scale video benchmark for human activity understanding," in *IEEE Int. Conf. on Computer Vision and Pattern Recognition*, 2015, pp. 961–970.
- [30] J. Barbič, A. Safonova, J.-Y. Pan, C. Faloutsos, J. K. Hodgins, and N. S. Pollard, "Segmenting motion capture data into distinct behaviors," in *Proceedings of Graphics Interface 2004*. Citeseer, 2004, pp. 185–194.
- [31] F. Zhou, F. De la Torre, and J. K. Hodgins, "Aligned cluster analysis for temporal segmentation of human motion," in *2008 8th IEEE international conference on automatic face & gesture recognition*. IEEE, 2008, pp. 1–7.
- [32] —, "Hierarchical aligned cluster analysis for temporal clustering of human motion," *IEEE Transactions on Pattern Analysis and Machine Intelligence*, vol. 35, no. 3, pp. 582–596, 2012.
- [33] S. Venkatesh, D. Moffat, and E. R. Miranda, "Investigating the effects of training set synthesis for audio segmentation of radio broadcast," *Electronics*, vol. 10, no. 7, p. 827, 2021.
- [34] E. B. Fox, M. C. Hughes, E. B. Sudderth, M. I. Jordan *et al.*, "Joint modeling of multiple time series via the beta process with application to motion capture segmentation," *The Annals of Applied Statistics*, vol. 8, no. 3, pp. 1281–1313, 2014.
- [35] D. Zhukov, J.-B. Alayrac, R. G. Cinbis, D. Fouhey, I. Laptev, and J. Sivic, "Cross-task weakly supervised learning from instructional videos," in *IEEE Int. Conf. on Computer Vision and Pattern Recognition*, 2019, pp. 3537–3545.
- [36] E. Elhamifar and Z. Naing, "Unsupervised procedure learning via joint dynamic summarization," in *Int. Conf. on Computer Vision*, 2019, pp. 6341–6350.
- [37] K. Zhang, W.-L. Chao, F. Sha, and K. Grauman, "Video summarization with long short-term memory," in *European Conf. on Computer Vision*. Springer, 2016, pp. 766–782.
- [38] C. Xu and E. Elhamifar, "Deep supervised summarization: Algorithm and application to learning instructions," in *Advances in Neural Information Processing Systems*, 2019, pp. 1109–1120.
- [39] Z. Naing and E. Elhamifar, "Procedure completion by learning from partial summaries," in *British Machine Vision Conference*, 2020.
- [40] N. Hussein, E. Gavves, and A. W. Smeulders, "Timeception for complex action recognition," in *IEEE Int. Conf. on Computer Vision and Pattern Recognition*, 2019, pp. 254–263.
- [41] —, "Pic: Permutation invariant convolution for recognizing long-range activities," *arXiv preprint arXiv:2003.08275*, 2020.
- [42] N. Hussein, M. Jain, and B. E. Bejnordi, "Timegate: Conditional gating of segments in long-range activities," *arXiv preprint arXiv:2004.01808*, 2020.
- [43] N. Hussein, E. Gavves, and A. W. Smeulders, "Videograph: Recognizing minutes-long human activities in videos," *arXiv preprint arXiv:1905.05143*, 2019.
- [44] M. Z. Shou, S. W. Lei, W. Wang, D. Ghadiyaram, and M. Feiszli, "Generic event boundary detection: A benchmark for event segmentation," in *Int. Conf. on Computer Vision*, 2021, pp. 8075–8084.
- [45] A. Fathi, X. Ren, and J. M. Rehg, "Learning to recognize objects in egocentric activities," in *IEEE Int. Conf. on Computer Vision and Pattern Recognition*, 2011.
- [46] S. Stein and S. J. McKenna, "Combining embedded accelerometers with computer vision for recognizing food preparation activities," in *ACM Int. Joint Conf. on Pervasive and Ubiquitous Computing*. ACM, 2013, pp. 729–738.
- [47] H. Kuehne, A. Arslan, and T. Serre, "The language of actions: Recovering the syntax and semantics of goal-directed human activities," in *IEEE Int. Conf. on Computer Vision and Pattern Recognition*, 2014.
- [48] F. Sener, D. Chatterjee, D. Shelepov, K. He, D. Singhanian, R. Wang, and A. Yao, "Assembly101: A large-scale multi-view video dataset for understanding procedural activities," in *IEEE Int. Conf. on Computer Vision and Pattern Recognition*, 2022, pp. 21 096–21 106.
- [49] L. Zhou, C. Xu, and J. J. Corso, "Towards automatic learning of procedures from web instructional videos," in *Thirty-Second AAAI Conference on Artificial Intelligence*, 2018.
- [50] Y. Tang, D. Ding, Y. Rao, Y. Zheng, D. Zhang, L. Zhao, J. Lu, and J. Zhou, "Coin: A large-scale dataset for comprehensive instructional video analysis," in *IEEE Int. Conf. on Computer Vision and Pattern Recognition*, 2019, pp. 1207–1216.
- [51] F. Ragusa, A. Furnari, S. Livatino, and G. M. Farinella, "The meccano dataset: Understanding human-object interactions from egocentric videos in an industrial-like domain," in *IEEE Winter Conf. on Applications of Computer Vision*, 2021, pp. 1569–1578.
- [52] Y. Ben-Shabat, X. Yu, F. Saleh, D. Campbell, C. Rodriguez-Opazo, H. Li, and S. Gould, "The ikea asm dataset: Understanding people assembling furniture through actions, objects and pose," in *IEEE Winter Conf. on Applications of Computer Vision*, 2021, pp. 847–859.
- [53] D. Fried, J.-B. Alayrac, P. Blunsom, C. Dyer, S. Clark, and A. Nematzadeh, "Learning to segment actions from observation and narration," in *Annual Meeting of the Association for Computational Linguistics*, 2020, pp. 2569–2588.
- [54] D. Damen, H. Doughty, G. M. Farinella, S. Fidler, A. Furnari, E. Kazakos, D. Moltisanti, J. Munro, T. Perrett, W. Price, and M. Wray, "Scaling egocentric vision: The epic-kitchens dataset," in *European Conf. on Computer Vision*, 2018.
- [55] D. Damen, H. Doughty, G. M. Farinella, A. Furnari, E. Kazakos, J. Ma, D. Moltisanti, J. Munro, T. Perrett, W. Price *et al.*, "Rescaling egocentric vision: collection, pipeline and challenges for epic-kitchens-100," *International Journal on Computer Vision*, vol. 130, no. 1, pp. 33–55, 2022.
- [56] Y. Li, M. Liu, and J. M. Rehg, "In the eye of beholder: Joint learning of gaze and actions in first person video," in *European Conf. on Computer Vision*, 2018, pp. 619–635.
- [57] J. Malmaud, J. Huang, V. Rathod, N. Johnston, A. Rabinovich, and K. Murphy, "What's cookin'? interpreting cooking videos using text, speech and vision," in *North American Chapter of the Association for Computational Linguistics (NAACL)*, 2015, pp. 143–152.
- [58] F. Sener and A. Yao, "Zero-shot anticipation for instructional activities," in *Int. Conf. on Computer Vision*, 2019, pp. 862–871.
- [59] Z. Liu, Z. Miao, X. Zhan, J. Wang, B. Gong, and S. X. Yu, "Large-scale long-tailed recognition in an open world," in *IEEE Int. Conf. on Computer Vision and Pattern Recognition*, 2019, pp. 2537–2546.

- [60] B. Kang, S. Xie, M. Rohrbach, Z. Yan, A. Gordo, J. Feng, and Y. Kalantidis, "Decoupling representation and classifier for long-tailed recognition," *arXiv preprint arXiv:1910.09217*, 2019.
- [61] C. Lea, M. D. Flynn, R. Vidal, A. Reiter, and G. D. Hager, "Temporal convolutional networks for action segmentation and detection," in *IEEE Int. Conf. on Computer Vision and Pattern Recognition*, 2017, pp. 156–165.
- [62] D. Singhania, R. Rahaman, and A. Yao, "Iterative contrast-classify for semi-supervised temporal action segmentation," in *Proceedings of the AAAI Conference on Artificial Intelligence*, vol. 36, no. 2, 2022, pp. 2262–2270.
- [63] G. Ding and A. Yao, "Leveraging action affinity and continuity for semi-supervised temporal action segmentation," in *European Conf. on Computer Vision*, 2022.
- [64] J. Li and S. Todorovic, "Action shuffle alternating learning for unsupervised action segmentation," in *IEEE Int. Conf. on Computer Vision and Pattern Recognition*, 2021, pp. 12 628–12 636.
- [65] R. Rahaman, D. Singhania, A. Thiery, and A. Yao, "A generalized & robust framework for timestamp supervision in temporal action segmentation," in *European Conf. on Computer Vision*, 2022.
- [66] G. Ding and A. Yao, "Temporal action segmentation with high-level complex activity labels," *IEEE Transactions on Multimedia*, 2022.
- [67] F. Sener and A. Yao, "Unsupervised learning and segmentation of complex activities from video," in *IEEE Int. Conf. on Computer Vision and Pattern Recognition*, 2018, pp. 8368–8376.
- [68] S. Sarfraz, N. Murray, V. Sharma, A. Diba, L. Van Gool, and R. Stiefelhagen, "Temporally-weighted hierarchical clustering for unsupervised action segmentation," in *IEEE Int. Conf. on Computer Vision and Pattern Recognition*, 2021, pp. 11 225–11 234.
- [69] Z. Du, X. Wang, G. Zhou, and Q. Wang, "Fast and unsupervised action boundary detection for action segmentation," in *IEEE Int. Conf. on Computer Vision and Pattern Recognition*, 2022, pp. 3323–3332.
- [70] C. Lea, A. Reiter, R. Vidal, and G. D. Hager, "Segmental spatiotemporal cnns for fine-grained action segmentation," in *European Conf. on Computer Vision*. Springer, 2016, pp. 36–52.
- [71] J. Li and S. Todorovic, "Set-constrained viterbi for set-supervised action segmentation," in *IEEE Int. Conf. on Computer Vision and Pattern Recognition*, 2020, pp. 10 820–10 829.
- [72] H. W. Kuhn, "The hungarian method for the assignment problem," *Naval research logistics quarterly*, vol. 2, no. 1-2, pp. 83–97, 1955.
- [73] T. Li and C. Ding, "The relationships among various nonnegative matrix factorization methods for clustering," in *Sixth International Conference on Data Mining (ICDM'06)*. IEEE, 2006, pp. 362–371.
- [74] J. Chang, Y. Guo, L. Wang, G. Meng, S. Xiang, and C. Pan, "Deep discriminative clustering analysis," *arXiv preprint arXiv:1905.01681*, 2019.
- [75] S. N. Aakur and S. Sarkar, "A perceptual prediction framework for self supervised event segmentation," in *IEEE Int. Conf. on Computer Vision and Pattern Recognition*, 2019, pp. 1197–1206.
- [76] A. Kukleva, H. Kuehne, F. Sener, and J. Gall, "Unsupervised learning of action classes with continuous temporal embedding," in *IEEE Int. Conf. on Computer Vision and Pattern Recognition*, 2019, pp. 12 066–12 074.
- [77] R. G. VidalMata, W. J. Scheirer, A. Kukleva, D. Cox, and H. Kuehne, "Joint visual-temporal embedding for unsupervised learning of actions in untrimmed sequences," in *IEEE Winter Conf. on Applications of Computer Vision*, 2021.
- [78] H. Wang, A. Kläser, C. Schmid, and C.-L. Liu, "Action recognition by dense trajectories," in *IEEE Int. Conf. on Computer Vision and Pattern Recognition*. IEEE, 2011, pp. 3169–3176.
- [79] H. Wang and C. Schmid, "Action recognition with improved trajectories," in *Int. Conf. on Computer Vision*, 2013, pp. 3551–3558.
- [80] F. Perronnin, J. Sánchez, and T. Mensink, "Improving the fisher kernel for large-scale image classification," in *European Conf. on Computer Vision*. Springer, 2010, pp. 143–156.
- [81] T. S. Jaakkola, D. Haussler *et al.*, "Exploiting generative models in discriminative classifiers," in *Advances in Neural Information Processing Systems*, 1999, pp. 487–493.
- [82] F. Perronnin and C. Dance, "Fisher kernels on visual vocabularies for image categorization," in *IEEE Int. Conf. on Computer Vision and Pattern Recognition*. IEEE, 2007, pp. 1–8.
- [83] H. Kuehne, J. Gall, and T. Serre, "An end-to-end generative framework for video segmentation and recognition," in *IEEE Winter Conf. on Applications of Computer Vision*. IEEE, 2016, pp. 1–8.
- [84] S. Ioffe and C. Szegedy, "Batch normalization: Accelerating deep network training by reducing internal covariate shift," in *Int. Conf. on Machine Learning*. PMLR, 2015, pp. 448–456.
- [85] W. Kay, J. Carreira, K. Simonyan, B. Zhang, C. Hillier, S. Vijayanarasimhan, F. Viola, T. Green, T. Back, P. Natsev *et al.*, "The kinetics human action video dataset," *arXiv preprint arXiv:1705.06950*, 2017.
- [86] C. Zach, T. Pock, and H. Bischof, "A duality based approach for realtime tv-l1 optical flow," in *Joint pattern recognition symposium*. Springer, 2007, pp. 214–223.
- [87] A. Richard, "Temporal segmentation of human actions in videos," Ph.D. dissertation, Universitäts-und Landesbibliothek Bonn, 2019.
- [88] T. Chen, S. Kornblith, M. Norouzi, and G. Hinton, "A simple framework for contrastive learning of visual representations," in *Int. Conf. on Machine Learning*. PMLR, 2020, pp. 1597–1607.
- [89] R. Qian, T. Meng, B. Gong, M.-H. Yang, H. Wang, S. Belongie, and Y. Cui, "Spatiotemporal contrastive video representation learning," in *IEEE Int. Conf. on Computer Vision and Pattern Recognition*, 2021, pp. 6964–6974.
- [90] G. Llorre, J. Rabarisoa, A. Orcesi, S. Ainouz, and S. Canu, "Temporal contrastive pretraining for video action recognition," in *IEEE Winter Conf. on Applications of Computer Vision*, 2020, pp. 662–670.
- [91] J. Choi, C. Gao, J. C. Messou, and J.-B. Huang, "Why can't i dance in the mall? learning to mitigate scene bias in action recognition," *Advances in Neural Information Processing Systems*, 2019.
- [92] D.-A. Huang, V. Ramanathan, D. Mahajan, L. Torresani, M. Paluri, L. Fei-Fei, and J. Carlos Niebles, "What makes a video a video: Analyzing temporal information in video understanding models and datasets," in *IEEE Int. Conf. on Computer Vision and Pattern Recognition*, 2018, pp. 7366–7375.
- [93] Y. Li and N. Vasconcelos, "Repair: Removing representation bias by dataset resampling," in *IEEE Int. Conf. on Computer Vision and Pattern Recognition*, 2019, pp. 9572–9581.
- [94] Y. Li, Y. Li, and N. Vasconcelos, "Resound: Towards action recognition without representation bias," in *European Conf. on Computer Vision*, 2018, pp. 513–528.
- [95] K. Cho, B. van Merriënboer, C. Gulcehre, D. Bahdanau, F. Bougares, H. Schwenk, and Y. Bengio, "Learning phrase representations using rnn encoder–decoder for statistical machine translation," in *Proceedings of the 2014 Conference on Empirical Methods in Natural Language Processing (EMNLP)*, 2014, pp. 1724–1734.
- [96] A. Richard, H. Kuehne, and J. Gall, "Weakly supervised action learning with rnn based fine-to-coarse modeling," in *IEEE Int. Conf. on Computer Vision and Pattern Recognition*, 2017.
- [97] Y. Huang, Y. Sugano, and Y. Sato, "Improving action segmentation via graph-based temporal reasoning," in *IEEE Int. Conf. on Computer Vision and Pattern Recognition*, 2020, pp. 14 024–14 034.
- [98] L. Ding and C. Xu, "Weakly-supervised action segmentation with iterative soft boundary assignment," in *IEEE Int. Conf. on Computer Vision and Pattern Recognition*, 2018, pp. 6508–6516.
- [99] P. Lei and S. Todorovic, "Temporal deformable residual networks for action segmentation in videos," in *IEEE Int. Conf. on Computer Vision and Pattern Recognition*, 2018, pp. 6742–6751.
- [100] D. Singhania, R. Rahaman, and A. Yao, "Coarse to fine multi-resolution temporal convolutional network," *arXiv preprint arXiv:2105.10859*, 2021.
- [101] O. Ronneberger, P. Fischer, and T. Brox, "U-net: Convolutional networks for biomedical image segmentation," in *International Conference on Medical image computing and computer-assisted intervention*. Springer, 2015, pp. 234–241.
- [102] S.-J. Li, Y. AbuFarha, Y. Liu, M.-M. Cheng, and J. Gall, "Mstcn++: Multi-stage temporal convolutional network for action segmentation," *IEEE Transactions on Pattern Analysis and Machine Intelligence*, 2020.
- [103] A. Vaswani, N. Shazeer, N. Parmar, J. Uszkoreit, L. Jones, A. N. Gomez, Ł. Kaiser, and I. Polosukhin, "Attention is all you need," in *Advances in Neural Information Processing Systems*, 2017, pp. 5998–6008.
- [104] G. Bertasius, H. Wang, and L. Torresani, "Is space-time attention all you need for video understanding?" in *Int. Conf. on Machine Learning*, vol. 2, no. 3, 2021, p. 4.

- [105] R. Girdhar, J. Carreira, C. Doersch, and A. Zisserman, "Video action transformer network," in *IEEE Int. Conf. on Computer Vision and Pattern Recognition*, 2019, pp. 244–253.
- [106] A. Arnab, M. Dehghani, G. Heigold, C. Sun, M. Lučić, and C. Schmid, "Vivit: A video vision transformer," in *Int. Conf. on Computer Vision*, 2021, pp. 6836–6846.
- [107] Z. Liu, Y. Lin, Y. Cao, H. Hu, Y. Wei, Z. Zhang, S. Lin, and B. Guo, "Swin transformer: Hierarchical vision transformer using shifted windows," in *Int. Conf. on Computer Vision*, 2021, pp. 10012–10022.
- [108] L. Zhu and Y. Yang, "Actbert: Learning global-local video-text representations," in *IEEE Int. Conf. on Computer Vision and Pattern Recognition*, 2020, pp. 8746–8755.
- [109] L. Li, Y.-C. Chen, Y. Cheng, Z. Gan, L. Yu, and J. Liu, "Hero: Hierarchical encoder for video+ language omni-representation pre-training," in *Proceedings of the 2020 Conference on Empirical Methods in Natural Language Processing (EMNLP)*, 2020, pp. 2046–2065.
- [110] F. Yi, H. Wen, and T. Jiang, "Asformer: Transformer for action segmentation," in *British Machine Vision Conference*, 2021.
- [111] N. Behrmann, S. A. Golestaneh, Z. Kolter, J. Gall, and M. Noroozi, "Unified fully and timestamp supervised temporal action segmentation via sequence to sequence translation," in *European Conf. on Computer Vision*, 2022.
- [112] F. Sener, D. Singhania, and A. Yao, "Temporal aggregate representations for long-range video understanding," in *European Conf. on Computer Vision*. Springer, 2020, pp. 154–171.
- [113] Y. Tang, X. Zhang, L. Ma, J. Wang, S. Chen, and Y.-G. Jiang, "Non-local netvlad encoding for video classification," in *European Conf. on Computer Vision*, 2018, pp. 0–0.
- [114] X. Zhu, W. Su, L. Lu, B. Li, X. Wang, and J. Dai, "Deformable detr: Deformable transformers for end-to-end object detection," *arXiv preprint arXiv:2010.04159*, 2020.
- [115] M. J. Powell, "A direct search optimization method that models the objective and constraint functions by linear interpolation," in *Advances in optimization and numerical analysis*. Springer, 1994, pp. 51–67.
- [116] A. Viterbi, "Error bounds for convolutional codes and an asymptotically optimum decoding algorithm," *IEEE transactions on Information Theory*, vol. 13, no. 2, pp. 260–269, 1967.
- [117] Y. Souri, Y. A. Farha, F. Despinoy, G. Francesca, and J. Gall, "Fifa: Fast inference approximation for action segmentation," in *DAGM German Conference on Pattern Recognition*. Springer, 2021, pp. 282–296.
- [118] D. Moltisanti, S. Fidler, and D. Damen, "Action recognition from single timestamp supervision in untrimmed videos," in *IEEE Int. Conf. on Computer Vision and Pattern Recognition*, 2019, pp. 9915–9924.
- [119] Z. Wang, Z. Gao, L. Wang, Z. Li, and G. Wu, "Boundary-aware cascade networks for temporal action segmentation," in *European Conf. on Computer Vision*, 2020.
- [120] Y. Ishikawa, S. Kasai, Y. Aoki, and H. Kataoka, "Alleviating over-segmentation errors by detecting action boundaries," in *IEEE Winter Conf. on Applications of Computer Vision*, 2021, pp. 2322–2331.
- [121] B. Singh, T. K. Marks, M. Jones, O. Tuzel, and M. Shao, "A multi-stream bi-directional recurrent neural network for fine-grained action detection," in *IEEE Int. Conf. on Computer Vision and Pattern Recognition*, 2016, pp. 1961–1970.
- [122] K.-N. C. Mac, D. Joshi, R. A. Yeh, J. Xiong, R. S. Feris, and M. N. Do, "Learning motion in feature space: Locally-consistent deformable convolution networks for fine-grained action detection," in *Int. Conf. on Computer Vision*, 2019, pp. 6282–6291.
- [123] H. Gammulle, T. Fernando, S. Denman, S. Sridharan, and C. Fookes, "Coupled generative adversarial network for continuous fine-grained action segmentation," in *IEEE Winter Conf. on Applications of Computer Vision*, 2019, pp. 200–209.
- [124] Y. Zhang, K. Muandet, Q. Ma, H. Neumann, and S. Tang, "Frontal low-rank random tensors for fine-grained action segmentation," *arXiv preprint arXiv:1906.01004*, 2019.
- [125] D. Wang, Y. Yuan, and Q. Wang, "Gated forward refinement network for action segmentation," *Neurocomputing*, vol. 407, pp. 63–71, 2020.
- [126] M.-H. Chen, B. Li, Y. Bao, and G. AlRegib, "Action segmentation with mixed temporal domain adaptation," in *IEEE Winter Conf. on Applications of Computer Vision*, 2020, pp. 605–614.
- [127] M.-H. Chen, B. Li, Y. Bao, G. AlRegib, and Z. Kira, "Action segmentation with joint self-supervised temporal domain adaptation," in *IEEE Int. Conf. on Computer Vision and Pattern Recognition*, 2020, pp. 9454–9463.
- [128] S.-H. Gao, Q. Han, Z.-Y. Li, P. Peng, L. Wang, and M.-M. Cheng, "Global2local: Efficient structure search for video action segmentation," in *IEEE Int. Conf. on Computer Vision and Pattern Recognition*, 2021, pp. 16805–16814.
- [129] S. Karaman, L. Seidenari, and A. Del Bimbo, "Fast saliency based pooling of fisher encoded dense trajectories," in *ECCV THUMOS Workshop*, vol. 1, no. 2, 2014, p. 5.
- [130] M. Rohrbach, S. Amin, M. Andriluka, and B. Schiele, "A database for fine grained activity detection of cooking activities," in *IEEE Int. Conf. on Computer Vision and Pattern Recognition*, 2012.
- [131] Y. Cheng, Q. Fan, S. Pankanti, and A. Choudhary, "Temporal sequence modeling for video event detection," in *IEEE Int. Conf. on Computer Vision and Pattern Recognition*, 2014, pp. 2227–2234.
- [132] A. Fathi, A. Farhadi, and J. M. Rehg, "Understanding egocentric activities," in *Int. Conf. on Computer Vision*, 2011, pp. 407–414.
- [133] A. Fathi and J. M. Rehg, "Modeling actions through state changes," in *IEEE Int. Conf. on Computer Vision and Pattern Recognition*, 2013, pp. 2579–2586.
- [134] N. N. Vo and A. F. Bobick, "From stochastic grammar to bayes network: Probabilistic parsing of complex activity," in *IEEE Int. Conf. on Computer Vision and Pattern Recognition*, 2014, pp. 2641–2648.
- [135] H. Pirsiavash and D. Ramanan, "Parsing videos of actions with segmental grammars," in *IEEE Int. Conf. on Computer Vision and Pattern Recognition*, 2014, pp. 612–619.
- [136] A. Richard and J. Gall, "Temporal action detection using a statistical language model," in *IEEE Int. Conf. on Computer Vision and Pattern Recognition*, 2016, pp. 3131–3140.
- [137] H. Kuehne, A. Richard, and J. Gall, "Weakly supervised learning of actions from transcripts," *Computer Vision and Image Understanding*, vol. 163, pp. 78–89, 2017.
- [138] P. Bojanowski, R. Lajugie, F. Bach, I. Laptev, J. Ponce, C. Schmid, and J. Sivic, "Weakly supervised action labeling in videos under ordering constraints," in *European Conf. on Computer Vision*, 2014.
- [139] Z. Lu and E. Elhamifar, "Weakly-supervised action segmentation and alignment via transcript-aware union-of-subspaces learning," in *Int. Conf. on Computer Vision*, 2021, pp. 8085–8095.
- [140] D.-A. Huang, L. Fei-Fei, and J. C. Niebles, "Connectionist temporal modeling for weakly supervised action labeling," in *European Conf. on Computer Vision*, 2016.
- [141] A. Graves, S. Fernández, F. Gomez, and J. Schmidhuber, "Connectionist temporal classification: labelling unsegmented sequence data with recurrent neural networks," in *Int. Conf. on Machine Learning*, 2006, pp. 369–376.
- [142] C.-Y. Chang, D.-A. Huang, Y. Sui, L. Fei-Fei, and J. C. Niebles, "D3tw: Discriminative differentiable dynamic time warping for weakly supervised action alignment and segmentation," in *IEEE Int. Conf. on Computer Vision and Pattern Recognition*, 2019, pp. 3546–3555.
- [143] J. Li, P. Lei, and S. Todorovic, "Weakly supervised energy-based learning for action segmentation," in *Int. Conf. on Computer Vision*, 2019, pp. 6243–6251.
- [144] Y. Souri, M. Fayyaz, L. Minciullo, G. Francesca, and J. Gall, "Fast weakly supervised action segmentation using mutual consistency," *IEEE Transactions on Pattern Analysis and Machine Intelligence*, 2021.
- [145] X. Chang, F. Tung, and G. Mori, "Learning discriminative prototypes with dynamic time warping," in *IEEE Int. Conf. on Computer Vision and Pattern Recognition*, 2021, pp. 8395–8404.
- [146] M. Fayyaz and J. Gall, "Sct: Set constrained temporal transformer for set supervised action segmentation," in *IEEE Int. Conf. on Computer Vision and Pattern Recognition*, 2020, pp. 501–510.
- [147] J. Li and S. Todorovic, "Anchor-constrained viterbi for set-supervised action segmentation," in *IEEE Int. Conf. on Computer Vision and Pattern Recognition*, 2021, pp. 9806–9815.
- [148] Z. Lu and E. Elhamifar, "Set-supervised action learning in procedural task videos via pairwise order consistency," in *IEEE Int. Conf. on Computer Vision and Pattern Recognition*, 2022, pp. 19903–19913.
- [149] Z. Li, Y. Abu Farha, and J. Gall, "Temporal action segmentation from timestamp supervision," in *IEEE Int. Conf. on Computer Vision and Pattern Recognition*, 2021, pp. 8365–8374.

- [150] H. Khan, S. Haresh, A. Ahmed, S. Siddiqui, A. Konin, M. Z. Zia, and Q.-H. Tran, "Timestamp-supervised action segmentation with graph convolutional networks," in *IROS*, 2022.
- [151] P. Bojanowski, R. Lajugie, E. Grave, F. Bach, I. Laptev, J. Ponce, and C. Schmid, "Weakly-supervised alignment of video with text," in *Int. Conf. on Computer Vision*, 2015, pp. 4462–4470.
- [152] O. Sener, A. R. Zamir, S. Savarese, and A. Saxena, "Unsupervised semantic parsing of video collections," in *Int. Conf. on Computer Vision*, 2015.
- [153] M. A. Fligner and J. S. Verducci, "Distance based ranking models," *Journal of the Royal Statistical Society. Series B (Methodological)*, pp. 359–369, 1986.
- [154] K. Goel and E. Brunskill, "Learning procedural abstractions and evaluating discrete latent temporal structure," in *Int. Conf. on Learning Representations*, 2019.
- [155] Z. Wang, H. Chen, X. Li, C. Liu, Y. Xiong, J. Tighe, and C. Fowlkes, "Sscap: Self-supervised co-occurrence action parsing for unsupervised temporal action segmentation," in *IEEE Winter Conf. on Applications of Computer Vision*, 2022, pp. 1819–1828.
- [156] S. Benaim, A. Ephrat, O. Lang, I. Mosseri, W. T. Freeman, M. Rubinstein, M. Irani, and T. Dekel, "Speednet: Learning the speediness in videos," in *IEEE Int. Conf. on Computer Vision and Pattern Recognition*, 2020, pp. 9922–9931.
- [157] K. Simonyan and A. Zisserman, "Very deep convolutional networks for large-scale image recognition," *arXiv preprint arXiv:1409.1556*, 2014.
- [158] S. Swetha, H. Kuehne, Y. S. Rawat, and M. Shah, "Unsupervised discriminative embedding for sub-action learning in complex activities," in *IEEE International Conference on Image Processing (ICIP)*. IEEE, 2021, pp. 2588–2592.
- [159] S. Kumar, S. Haresh, A. Ahmed, A. Konin, M. Z. Zia, and Q.-H. Tran, "Unsupervised action segmentation by joint representation learning and online clustering," in *IEEE Int. Conf. on Computer Vision and Pattern Recognition*, 2022, pp. 20 174–20 185.
- [160] S. Bansal, C. Arora, and C. Jawahar, "My view is the best view: Procedure learning from egocentric videos," in *European Conf. on Computer Vision*, 2022.
- [161] X. Chen, S. Xie, and K. He, "An empirical study of training self-supervised vision transformers," in *Int. Conf. on Computer Vision*, 2021, pp. 9640–9649.
- [162] B. Soran, A. Farhadi, and L. Shapiro, "Generating notifications for missing actions: Don't forget to turn the lights off!" in *Int. Conf. on Computer Vision*, 2015, pp. 4669–4677.
- [163] D. Rivoir, S. Bodenstedt, F. von Bechtolsheim, M. Distler, J. Weitz, and S. Speidel, "Unsupervised temporal video segmentation as an auxiliary task for predicting the remaining surgery duration," in *OR 2.0 Context-Aware Operating Theaters and Machine Learning in Clinical Neuroimaging*. Springer, 2019, pp. 29–37.
- [164] Y. A. Farha, A. Richard, and J. Gall, "When will you do what? Anticipating temporal occurrences of activities," in *IEEE Int. Conf. on Computer Vision and Pattern Recognition*, 2018.
- [165] Q. Ke, M. Fritz, and B. Schiele, "Time-conditioned action anticipation in one shot," in *IEEE Int. Conf. on Computer Vision and Pattern Recognition*, 2019.
- [166] H. Gammulle, S. Denman, S. Sridharan, and C. Fookes, "Forecasting future action sequences with neural memory networks," in *British Machine Vision Conference*, 2019.
- [167] E. Apostolidis, E. Adamantidou, A. I. Metsai, V. Mezaris, and I. Patras, "Video summarization using deep neural networks: A survey," *Proceedings of the IEEE*, vol. 109, no. 11, pp. 1838–1863, 2021.
- [168] R. Ghoddoosian, I. Dwivedi, N. Agarwal, C. Choi, and B. Darius, "Weakly-supervised online action segmentation in multi-view instructional videos," in *IEEE Int. Conf. on Computer Vision and Pattern Recognition*, 2022, pp. 13 780–13 790.